Journal of Medicinal Chemistry

Subscriber access provided by UNIV AUTONOMA DE COAHUILA UADEC

Article

Discovery of Pyrrolo[3,2-d]pyrimidin-4-one Derivatives as a New Class of Potent and Cell Active Inhibitors of P300/CBP-Associated Factor Bromodomain

Lu-Yi Huang, Hui Li, Lin-Li Li, Lu Niu, Raina Seupel, Chengyong Wu, Wei Cheng, Chong Chen, Bisen Ding, Paul E Brennan, and Shengyong Yang

J. Med. Chem., **Just Accepted Manuscript** • DOI: 10.1021/acs.jmedchem.9b00096 • Publication Date (Web): 18 Apr 2019

Downloaded from http://pubs.acs.org on April 18, 2019

Just Accepted

"Just Accepted" manuscripts have been peer-reviewed and accepted for publication. They are posted online prior to technical editing, formatting for publication and author proofing. The American Chemical Society provides "Just Accepted" as a service to the research community to expedite the dissemination of scientific material as soon as possible after acceptance. "Just Accepted" manuscripts appear in full in PDF format accompanied by an HTML abstract. "Just Accepted" manuscripts have been fully peer reviewed, but should not be considered the official version of record. They are citable by the Digital Object Identifier (DOI®). "Just Accepted" is an optional service offered to authors. Therefore, the "Just Accepted" Web site may not include all articles that will be published in the journal. After a manuscript is technically edited and formatted, it will be removed from the "Just Accepted" Web site and published as an ASAP article. Note that technical editing may introduce minor changes to the manuscript text and/or graphics which could affect content, and all legal disclaimers and ethical guidelines that apply to the journal pertain. ACS cannot be held responsible for errors or consequences arising from the use of information contained in these "Just Accepted" manuscripts.

ACS Publications

is published by the American Chemical Society. 1155 Sixteenth Street N.W., Washington, DC 20036

Published by American Chemical Society. Copyright © American Chemical Society. However, no copyright claim is made to original U.S. Government works, or works produced by employees of any Commonwealth realm Crown government in the course of their duties.

Discovery of Pyrrolo[3,2-d]pyrimidin-4-one Derivatives as a New Class of Potent and Cell Active Inhibitors of P300/CBP-Associated Factor Bromodomain

Luyi Huang,[†,#] Hui Li,[†,#] Linli Li,[‡,#] Lu Niu,[†] Raina Seupel,[§] Chengyong Wu,[†] Wei Cheng,[†] Chong Chen,[†] Bisen Ding,[†] Paul E. Brennan,[§] Shengyong Yang[†,*]

[†]State Key Laboratory of Biotherapy and Cancer Center, West China Hospital, Sichuan University, Chengdu 610041, P.R. China.

[‡]Key Laboratory of Drug Targeting and Drug Delivery System of Ministry of Education, West China School of Pharmacy, Sichuan University, Sichuan 610041, P.R. China

[§]Structural Genomics Consortium & Target Discovery Institute, University of Oxford, NDM Research Building Roosevelt Drive, Oxford, OX3 7DQ and OX3 7FZ, United Kingdom

[#]These authors contributed equally to this work.

*To whom correspondence should be addressed. Shengyong Yang, State Key Laboratory of Biotherapy and Cancer Center, West China Hospital, Sichuan University, Chengdu, Sichuan 610041, China. E-mail: yangsy@scu.edu.cn.

ABSTRACT

Herein we report the discovery of a series of new PCAF bromodomain (BRD) inhibitors, which were obtained through a hit discovery process and subsequent structure-based optimization and structure-activity relationship (SAR) analyses towards a retrieved hit compound (**12**). Among these inhibitors, (*R,R*)-**36n** is the most potent one with an IC_{50} of 7 nM in HTRF assay and a K_D of 78 nM in ITC assay. This compound also exhibited activity against GCN5 and FALZ, but weak or no activity against other 29 BRD proteins and 422 kinases, indicating considerable selectivity. X-ray cocrystal structure analysis revealed the molecular interaction mode and the precise stereochemistry required for bioactivity. Cellular activity, preliminary RNA-seq analysis and pharmacokinetic properties were also examined for this compound. Collectively, this study provides a versatile tool molecule to explore molecular mechanisms of PCAF BRD regulation and also offers a new lead compound for drug discovery targeting PCAF.

1. INTRODUCTION

Bromodomains (BRDs) are highly conserved epigenetic "reader" protein modules that recognize ε-*N*-acetylated lysine marks on proteins,[1] and play a key role in the epigenetic regulation of gene transcription. A total of 61 BRDs are identified in the human proteome, which present in 46 diverse proteins.[2] Among these BRDs, BET (Bromo and extra-terminal) BRDs are the most extensively studied subfamily (subfamily Ⅱ of BRD phylogenetic tree). A large number of selective and potent BET BRD inhibitors have been discovered,[3, 4] which have provided versatile tools for bio-functional studies, and further led to numerous translational studies on this subfamily of BRD proteins.[5-9] In contrast, BRDs in non-BET subfamilies have received less attention. Biological functions of many non-BET BRDs in physiological and pathological conditions are still not clear, and inhibitors of these BRDs are also much less.[10-12]

P300/CBP-associated factor (PCAF), also known as lysine acetyltransferase 2B (KAT2B), is a BRD-containing protein, which belongs to subfamily I of the BRD phylogenetic tree.[1] PCAF is a multidomain protein including an acetyltransferase (HAT) domain,[13] a *N*-terminal E3 ubiquitin ligase domain,[14] and a C-terminal bromodomain,[15] which has been implicated in a number of disparate disease pathologies and small molecule modulators have great potential as therapeutics.[16] Regulation mechanisms and roles in diseases of these domains, particularly the C-terminal bromodomain, are far from understood. Small molecule inhibitors might provide tool molecules to unravel the functions of the PCAF BRD on the one hand, on the other hand, offer potential lead compounds for drug development targeting PCAF BRD.

To date, a number of small molecular inhibitors of PCAF BRD have been reported, which are summarized in Figure 1. Zeng et al. reported the first PCAF inhibitor **1**, which could disrupt the PCAF-BRD/Tat-AcK50 interaction in vitro.[17] Subsequent structural

optimization of **1** generated a more potent compound **2**.[18] Navratilova et al.[19] and Chaikuad et al.[20] separately used fragment-based screening approaches to identify PCAF BRD inhibitors, and a number of inhibitors (fragments) were retrieved, for example, compound **3** and **4**. In 2016, Genentech and Constellation disclosed potent dual PCAF/GCN5 BRDs inhibitors in three patents, and compounds **5-7** shown in Figure 1 are representative ones although no selectivity data was reported.[21-23] Later, Brennan and coworkers reported a [1,2,4]triazolo[3,4-a]phthalazine derivative, **8 (*L*-Moses**, Figure 1) as a potent, selective, and cell active PCAF probe.[24] Researchers from GlaxoSmithKline published a potent PCAF/GCN5 BRDs inhibitor **9**,[25] and very recently, they further derived a PROTAC compound (GSK699) from **9**.[26]

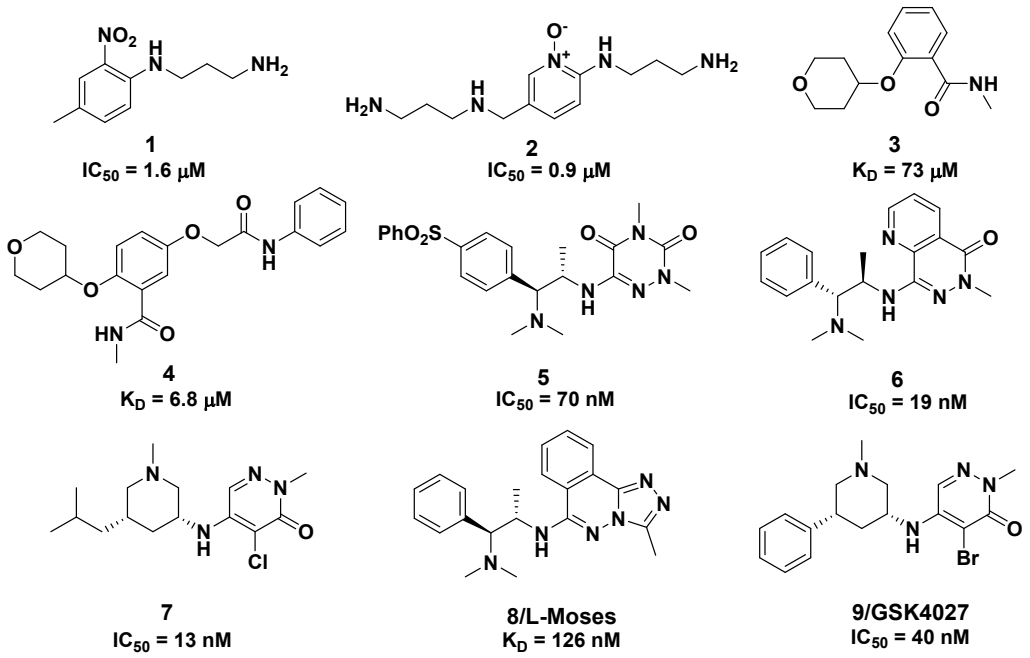

Figure 1. Representative PCAF BRD inhibitors publicly reported.

Despite these recent advances, there are still very few reported potent and selective PCAF BRD inhibitors. The aim of this investigation was to identify more novel potent and selective PCAF BRD inhibitors. To achieve this goal, we first performed virtual screening (VS) against an in-house chemical database to retrieve hit compounds, which

led to the discovery of three hits. The most potent hit compound, which contains a new pyrrolo[3,2-d]pyrimidin-4-one scaffold, was then selected for subsequent structural optimization. Structure-activity relationship (SAR) analyses resulted in the discovery of a series of new PCAF BRD inhibitors containing the scaffold pyrrolo[3,2-d]pyrimidin-4-one. For the most active compound, further investigations including selectivity profiling, ligand-receptor interaction analysis, cellular activity, preliminary RNA-seq (RNA-sequencing) analysis and pharmacokinetic studies were carried out.

2. RESULTS AND DISCUSSION

2.1. Retrieving of Hit Compounds

To discover more potent PCAF BRD inhibitors with new scaffolds, we first conducted a virtual screening (VS) study against an in-house chemical database (details for the VS see Supporting Information Figure S1). Selected hit compounds in VS were then subjected to a differential scanning fluorimetry (DSF) assay at a compound concentration of 20 μM. Compounds with a thermal shift (ΔT_m) of ≥ 1 °C in the DSF assay were then validated by isothermal titration calorimetry (ITC) assay. We finally obtained three weakly active compounds, **10**, **11**, and **12**, which showed K_D values of 45, 7.8 and 2.4 μM in the ITC assay, respectively (Figure 2). Compound **10** shows some similarity to previously reported BRD7/9,[27] BAZ2A/B,[28] and CBP/EP300[29, 30] BRD inhibitors and compound **11** contains the previously reported phthalazinone scaffold,[22] but compound **12** harbors a new scaffold, pyrrolo[3,2-d]pyrimidin-4-one, which has not been reported previously in BRD inhibitors. We chose compound **12** to conduct further structural optimization because it is the most potent compound and has a novel scaffold.

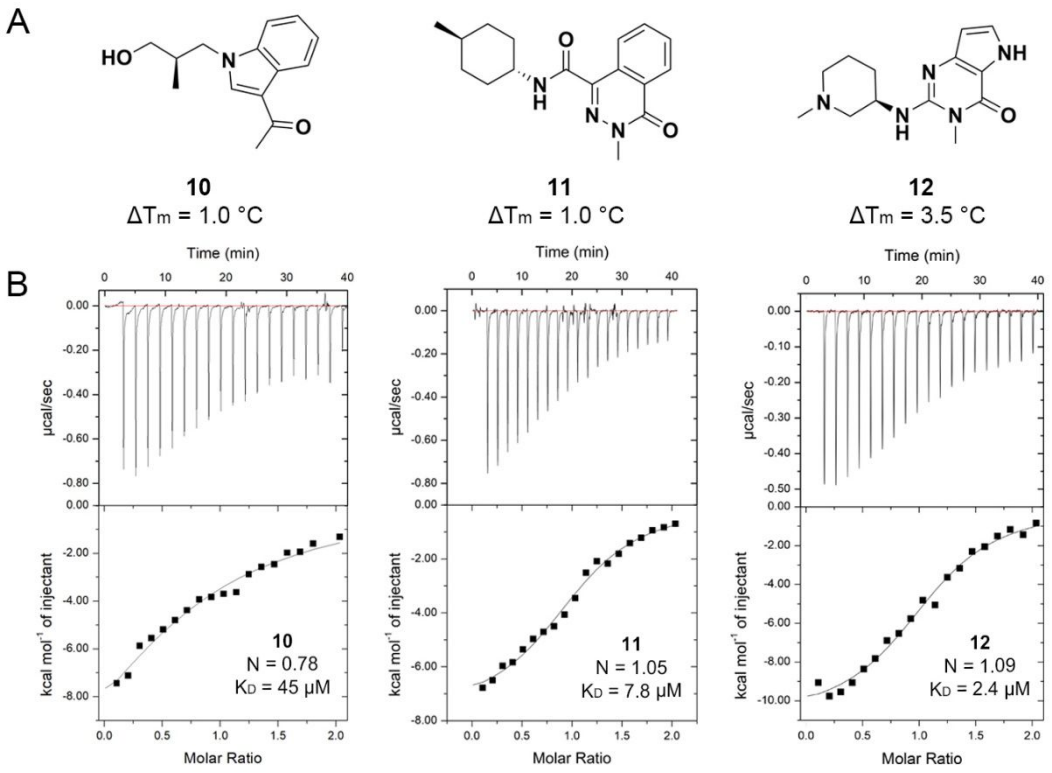

Figure 2. Three active compounds found by VS and subsequent bioactivity evaluation. (A) Chemical structures of **10**, **11**, and **12**. (B) Isothermal titration data of the interaction of hit compounds (for **10** and **11**, 500 µM ligand and 50 µM PCAF BRD were used; for **12**, 200 µM ligand and 20 µM PCAF were used) with PCAF BRD.

To facilitate the following structural optimization of **12**, an X-ray cocrystal structure of PCAF in complex with **12** was solved with a resolution of 2.1 Å resolution (PDB ID: 6J3O). As shown in Figure 3, compound **12** bound to the acetyllysine-binding site and had well defined by electron density. This compound forms hydrogen bonds with four amino acids, Pro747, Asn803, Tyr760, and Tyr809, either directly or via water-mediated interaction. The methyl substituent at the 3-position was in the water channel occupied by the acetyl lysine of the histone ligand. We also observed a π-π stacking interaction between the pyrrolo[3,2-d]pyrimidin-4-one core and the benzene ring of Tyr809. The basic piperidine group forms a salt bridge with acidic side chain of

Glu756, which is further stabilized by the backbone amide nitrogen of Lys753 through a hydrogen bond. Here it is necessary to mention that compound **12** seems to make the same interactions with PCAF BRD as compound (*R*)-**23** in reference 25, and the only difference is that compound **12** forms an additional hydrogen bond with Asn803.

2.2. Structural Optimization and SAR Analyses of Pyrrolo[3,2-d]pyrimidin-4-one Derivatives

Structural optimization of hit compound **12** was focused on three regions, namely, the 2-amino moiety (region Ⅰ), the 3-position (region Ⅱ) and the 5-position substituent (region Ⅲ) of pyrrolo[3,2-d]pyrimidin-4-one (Figure 3C). A number of new pyrrolo[3,2-d]pyrimidin-4-one derivatives were designed and synthesized. Bioactivities of these compounds against PCAF BRD were measured by DSF and ITC assays.

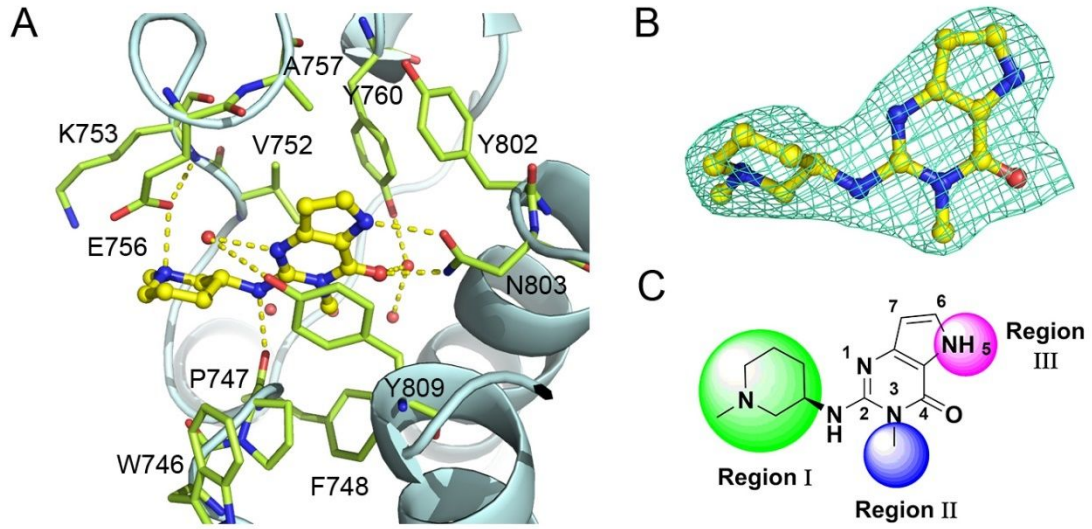

Figure 3. Cocrystal structure of PCAF/**12** guided the structural optimization. (A) Cocrystal structure of compound **12** (yellow sticks) in complex with PCAF bromodomain (pale cyan cartoon) (PDB ID: 6J3O). Related residues are shown as

green sticks. (B) Experimental electron density map ($2F_o$-F_c) contoured at 1σ around the hit **12**. (C) Focused regions in the structural optimization and SAR analyses.

2.2.1. Impact of 2-Amino Moiety (Region I)

To explore the impact of 2-amino moiety of compound **12** on the bioactivity, we varied region Ⅰ and fixed region Ⅱ and Ⅲ with their original substituents. According to the cocrystal structure of **12**-PCAF complex (Figure 3A), the basic *N*-methyl piperidine in region I, which forms a salt bridge with acidic Glu756, plays an important role to the ligand-receptor interaction. But the *N*-methyl piperidine group is not large enough to occupy the ZA channel. Accordingly, all substituents used in region I were required to contain a secondary or tertiary amine, and larger than *N*-methyl piperidine to make potential interactions with Trp746 and Lys753. Based on this observation and inspiration from the SAR study of compound **9**,[25] we designed and synthesized a total of 10 compounds ((*R,R*)-**24a**, (*S,S*)-**24a**, *cis*-**24b**, *endo*-**24c-e**, *endo*-**25a**, *exo*-**25a**, and *endo*-**26a-b).**

Scheme 1 shows synthetic routes for these compounds. Commercially available 2,4-dichloro-5H-pyrrolo[3,2-d]pyrimidine (**13**) underwent alkaline hydrolysis to produce intermediate **14**. Boc-protection of **14** gave **15**. Subsequent methylation and Boc-deprotection of **15** generated the key intermediate **16**. (*R*)/(*S*)-**17a** or **17b** (racemate) reacted with picolinic acid to produce (*R*)/(*S*)-**18a** or **18b**, which underwent C(sp^3)-H arylation with iodobenzene to afford enantiomerically pure (*R,R*)/(*S,S*)-**19a** or *cis*-**19b**, respectively.[31] Compounds (*R,R*)/(*S,S*)-**19a** and *cis*-**19b** were further converted to (*R,R*)/(*S,S*)-**20a** and *cis*-**20b** by Boc-deprotection, reductive amination and subsequent alkaline hydrolysis. (*R,R*)/(*S,S*)-**20a** and *cis*-**20b** together with two commercially available amines **21-22** were subjected to a tractable S_NAr reaction with **16** to afford

target products (*R,R*)-**24a**, (*S,S*)-**24a**, *cis*-**24b**, and *endo*-**24c-d**. **23** (*endo*/*exo* mixture) reacted with **16** to afford *endo*- and *exo*-**24e**. Acidic *N*-deprotection of *endo*- and *exo*-**24e** afforded *endo*- and *exo*-**25a**, respectively. *N*-alkylation of *endo*-**25a** with (*R*)-2-phenyloxirane or (*R*)-2-bromo-1-(pyridin-2-yl)ethan-1-ol produced *endo*-**26a-b**.

Scheme 1. Synthesis of (*R,R*)-**24a**, (*S,S*)-**24a**, *cis*-**24b**, *endo*-**24c-e**, *endo*-**25a**, *exo*-**25a**, and *endo*-**26a-b** [a]

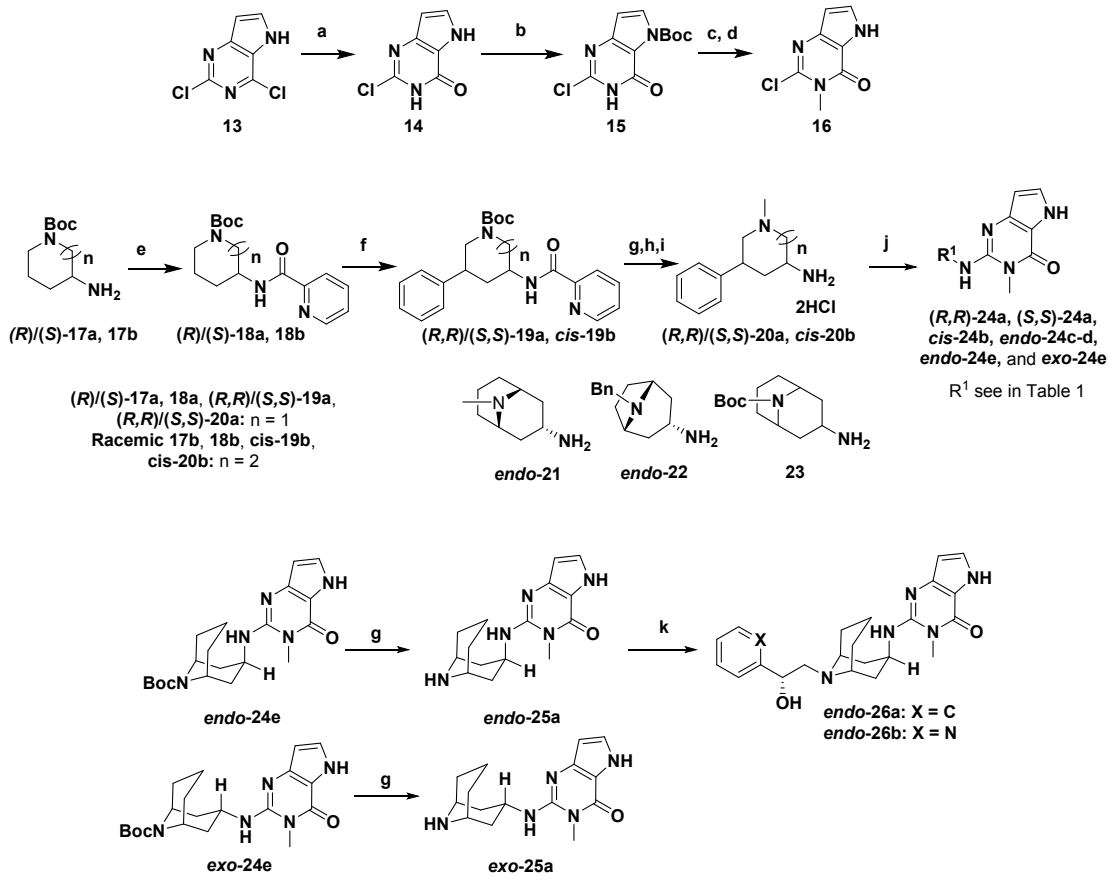

[a] Reagents and conditions: (a) 1M NaOH (aq), 100 °C, 16 h, 90%; (b) Boc_2O, TEA, DMAP, DMF, rt, 82%; (c) iodomethane, NaH, anhydrous DMF, 40 °C, overnight; (d) trifluoroacetic acid, DCM, rt, 46% over two steps; (e) picolinic acid, HATU, DIPEA, DCM, rt, 83-88%; (f) iodobenzene, $Pd(OAc)_2$, Ag_2CO_3, 2,6-dimethylbenzoic acid, *t*-BuOH, 120 °C, 24 h, 62-77%, > 99% *ee*; (g) trifluoroacetic acid, DCM, rt; (h) 37% formaldehyde, $NaBH(OAc)_3$, AcOH, DCM, rt, 8 h, 84%; (i) NaOH, *i*-PrOH, 85 °C, 18

h, 78-85%; (j) **16**, primary amines, DIPEA, NMP, 150 °C, 2-5 h, 12-37%; (k) (*R*)-2-phenyloxirane or (*R*)-2-bromo-1-(pyridin-2-yl)ethan-1-ol, TEA, MeCN, 70 °C, overnight, 47-58%.

The synthesized compounds were assayed against the PCAF BRD and bioactivities of these compounds are presented in Table 1. (*R,R*)-**24a**, containing a (*R,R*)-1-methyl-5-phenylpiperidin-3-amino group, showed a thermal shift (ΔT_m) of 6.3 °C in DSF assay, and a K_D of 152 nM in ITC assay, whereas its enantiomer (*S,S*)-**24a** lost activity. *Cis*-**24b** with piperidine in (*R,R*)-**24a** replaced by azacycloheptane also displayed considerable activity in both assays (ΔT_m = 3.2 °C and K_D = 347 nM), but relatively weaker potency compared with those of (*R,R*)-**24a.** Among the remaining seven compounds containing a bridged piperidine, *endo*-**24c** was the most potent one (ΔT_m =7.3 °C and K_D = 0.215 μM). The *N*-methyl removal product *endo*-**25a** slightly decreased in bioactivity (ΔT_m = 6.6 °C and K_D = 0.242 μM), whereas the diastereomer *exo*-**25a** did not exhibit activity. *Endo*-**24e**, *endo*-**26a**, and *endo*-**26b** with a bulky substituent in the bridged piperidine displayed a significant reduced activity in both assays. *Endo*-**24d**, which contains a 2-carbon-bridged piperidine (tropane), showed no activity.

Table 1. Bioactivities of Region I Substituted Compounds against PCAF BRD.

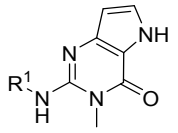

Compd	R^1	K_D (μM)	ΔT_m (°C)[a]

(*R,R*)-**24a**	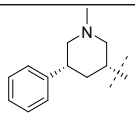	0.152	6.3 ± 0.6
(*S,S*)-**24a**	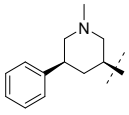	> 10	0.6 ± 0.2
cis-**24b**	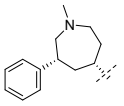	0.347	3.2 ± 0.3
endo-**24c**		0.215	7.3 ± 0.4
endo-**24d**	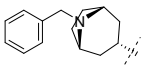	> 10	0.4 ± 0.4
endo-**24e**	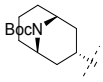	2.16	1.7 ± 0.5
endo-**25a**		0.242	6.6 ± 0.2
exo-**25a**		> 10	1.0 ± 0.2
endo-**26a**	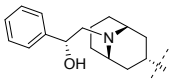	0.935	3.6 ± 1.0
endo-**26b**	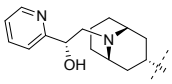	1.19	4.6 ± 0.3

[a] Values are averages of triplicates ± SEM (2 μM PCAF, 10 μM compound).

2.2.2. Influence of 3- and 5-Position Substitutions (Region Ⅱ and Ⅲ).

To examine the influence of 3- and 5-position substitutions of pyrrolo[3,2-d]pyrimidin-4-one core, we fixed 2-position (region Ⅰ) with its optimal group, (*R,R*)-1-methyl-5-phenylpiperidin-3-amino, and varied the 3- or 5-position substituents. Six new compounds ((*R,R*)-**32a-f**) were designed and synthesized (Scheme 2); for the 3-position substituents, we introduced unsaturated alkyl groups because it has been

reported that unsaturated alkyl groups at this position might influence the bioactivity or selectivity across bromodomains.[32] Intermediate **15** underwent an alkylation reaction with various haloalkanes followed by Boc-deprotection gave **27a-d**. Methylation of **14** with methyl iodide afforded **28**. Selective hydrolysis of **29** with 1 M NaOH generated **30**, and methylation of **30** resulted in the formation of **31** in an excellent yield. Finally, **27a-d**, **28**, and **31** reacted with (*R,R*)-**20a** to produce (*R,R*)-**32a-f**, respectively.

Scheme 2. Synthesis of (*R,R*)-**32a-f**[a]

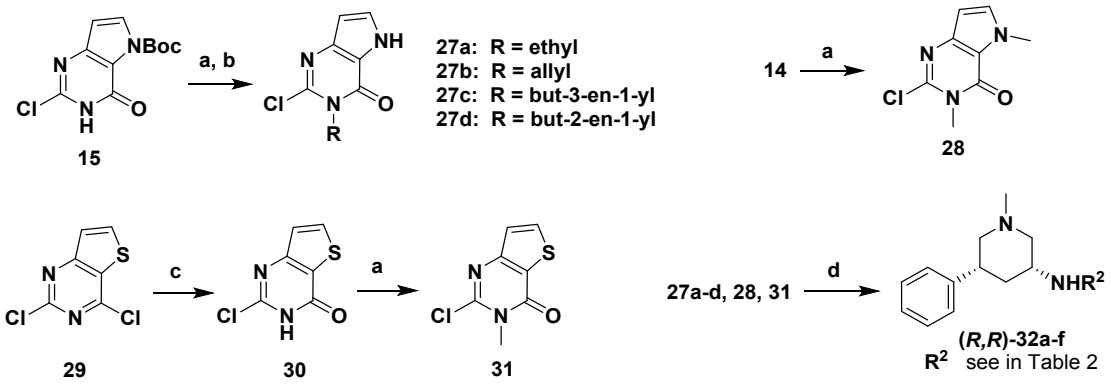

[a]Reagents and conditions: (a) haloalkanes, NaH, anhydrous DMF, 50 °C, overnight, 34-78%; (b) trifluoroacetic acid, DCM, rt; (c) 1M NaOH (aq), 100 °C, 95%; (d) (*R,R*)-**20a**, DIPEA, NMP, 150 °C, 2 h, 13-47%.

Table 2 shows the bioactivities of these compounds. From Table 2, we can see that the longer the (unsaturated) alkyl chain of 3-position, the worse the bioactivity ((*R,R*)-**32a-d**), indicating that a bulky group at 3-position is unfavorable for bioactivity. To explore the impact of 5-position substitution of pyrrolo[3,2-d]pyrimidin-4-one, we firstly added a methyl group at 5-position. Bioactivity of the resulting compound (*R,R*)-**32e** decreased significantly, implying that the hydrogen bond (NH…O) is important and substitution at this position is not favored (see Figure 3A). Displacing the nitrogen

atom on 5-position with a sulfur atom ((*R,R*)-**32f**) also decreased the binding affinity, demonstrated again the importance of the hydrogen bond (NH…O).

Table 2. Bioactivities of Compounds (*R,R*)-**32a-f** against PCAF BRD.

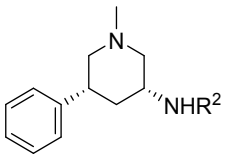

Compd	R^2	K_D (μM)	ΔT_m (°C)[a]
(*R,R*)-**32a**	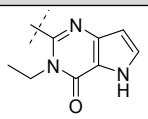	0.621	4.8 ± 0.2
(*R,R*)-**32b**	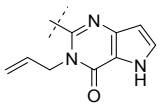	0.676	2.2 ± 0.6
(*R,R*)-**32c**	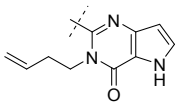	3.41	1.5 ± 0.4
(*R,R*)-**32d**	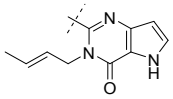	3.04	1.5 ± 0.4
(*R,R*)-**32e**	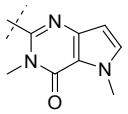	> 10	-0.2 ± 0.4
(*R,R*)-**32f**	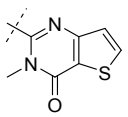	0.820	4.6 ± 0.4

[a] Values are averages of triplicates ± SEM (2 μM PCAF, 10 μM compound).

2.2.3. Effect of Various Substituted 3-Amino-5-phenylpiperidine (Region I)

In preceding structural optimization, we obtained a potent compound, (*R,R*)-**24a**. SAR analyses indicated that any changes in region II and III were not favored for bioactivity improvement. We thus turned back to recheck region I, and examined the

possible effect of various substituents on the piperidine ring (R^3 and R^4). Fifteen compounds ((*R,R*)-**36a-n** and (*S,S*)-**36n**) were synthesized.

Scheme 3 outlines the reaction routes for these compounds. Compound (*R,R*)- or (*S,S*)-**18a** reacted with various aryl iodides via C(sp^3)-H arylation to afford enantiomerically pure (*R,R*)-**19a**, (*R,R*)-**33a-j** and (*S,S*)-**19a**.[31] Compounds (*R,R*)-**19a**, (*R,R*)-**33a-j** and (*S,S*)-**19a** were further converted to (*R,R*)-**34a-m** and (*S,S*)-**34m** by Boc-deprotection and subsequent reductive amination or nucleophilic substitution. Cleavage of the bidentate directing groups of (*R,R*)-**34a-m** and (*S,S*)-**34m** with the use of NaOH/*i*-PrOH resulted in amines (*R,R*)-**35a-m** and (*S,S*)-**35m**, which were subjected to S_NAr reaction with **16** to afford target products (*R,R*)-**36a-i**, (*R,R*)-**36k-n**, and (*S,S*)-**36n**. Pd/C catalyzed debenzylation of (*R,R*)-**36i** produced (*R,R*)-**36j**.

Scheme 3. Synthesis of Compounds (*R,R*)-**36a-n** and (*S,S*)-**36n**[a]

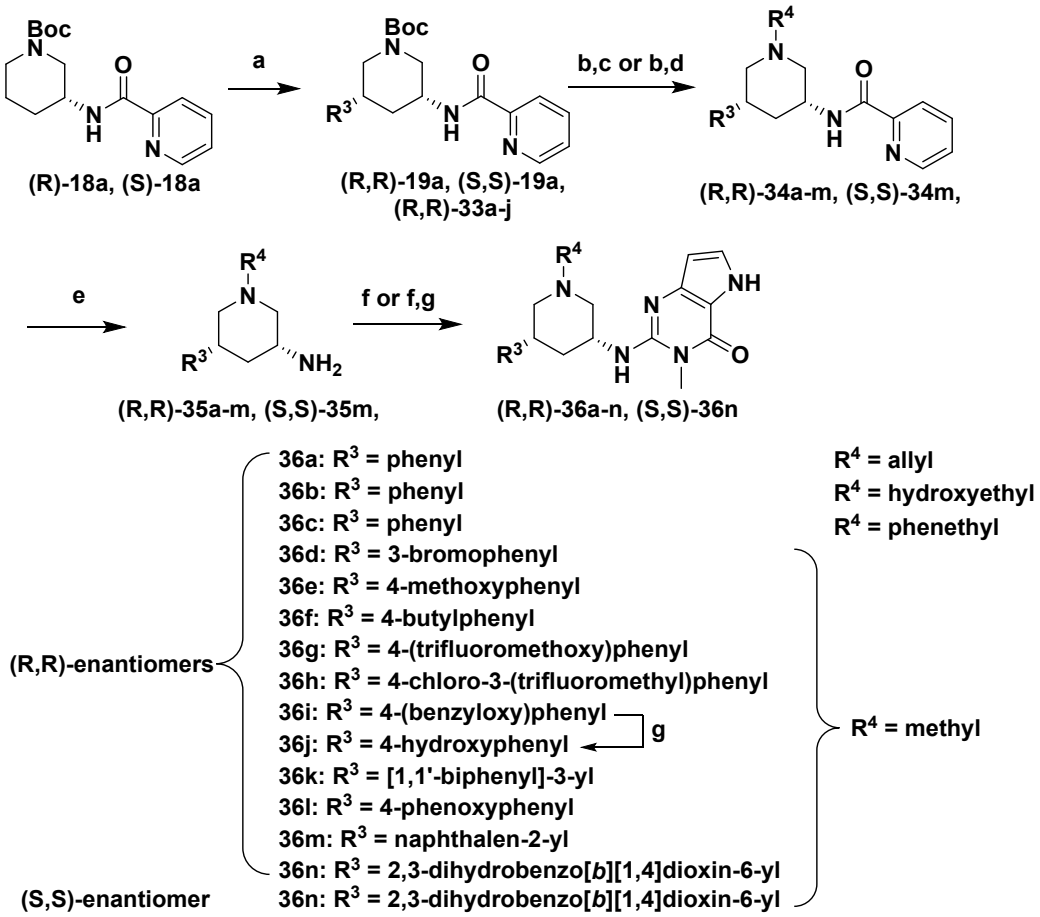

[a] Reagents and conditions: (a) aryl iodides, $Pd(OAc)_2$, Ag_2CO_3, 2,6-dimethylbenzoic acid, *t*-BuOH, 120 °C, 24 h, 52-76%, > 99% *ee*; (b) trifluoroacetic acid, DCM, rt; (c) haloalkanes, TEA, MeCN, 80 °C, overnight, 76%; (d) 37% formaldehyde (aq), $NaBH(OAc)_3$, AcOH, DCM, rt, 73%; (e) NaOH, *i*-PrOH, 85 °C, 18 h; (f) **16**, DIPEA, NMP, 150 °C, 2 h, 11-26%; (g) (*R,R*)-**36i**, 10% Pd/C, H_2, MeOH, rt, 65%.

Bioactivities of these compounds are shown in Table 3. Increasing the size of *N*-alkyl substituent (R^4) from methyl to allyl ((*R,R*)-**36a**), hydroxyethyl ((*R,R*)-**36b**), and phenethyl ((*R,R*)-**36c**) decreased the bioactivity. Meta- and/or para-substituted phenyl groups at R^3 ((*R,R*)-**36d-l**) delivered potent activities, which are comparable to those of (*R,R*)-**24a**. (*R,R*)-**36m**, bearing a naphthalene-2-yl, enhanced the activity (K_D: 0.103 μM). (*R,R)*-**36n** with R^3 substituted by 2,3-dihydro-1,4-benzodioxin-6-yl showed the

most potent activity among all the synthesized compounds (K_D: 0.078 μM, ΔT_m: 9.5 °C) (Figure 4A and 4C). Of special note is that the enantiomer (*S,S*)-**36n** showed no obvious activity.

Table 3. Bioactivities of Compounds (*R,R*)-**36a-n** and (*S,S*)-**36n** against PCAF BRD

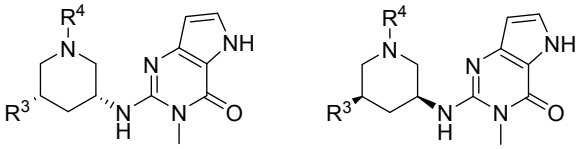

(*R,R*)-**36a-n** (*S,S*)-**36n**

Compd	R^3	R^4	K_D (μM)	ΔT_m (°C)[a]
(*R,R*)-**36a**			0.233	4.4 ± 0.3
(*R,R*)-**36b**		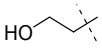	0.535	4.7 ± 0.3
(*R,R*)-**36c**		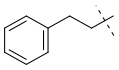	1.20	2.5 ± 0.7
(*R,R*)-**36d**	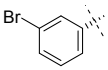	CH_3	0.128	7.5 ± 0.4
(*R,R*)-**36e**	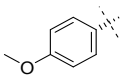	CH_3	0.106	8.0 ± 0.4
(*R,R*)-**36f**	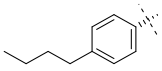	CH_3	0.183	4.6 ± 0.9
(*R,R*)-**36g**	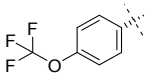	CH_3	0.140	5.9 ± 0.3
(*R,R*)-**36h**	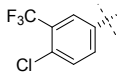	CH_3	0.138	6.6 ± 0.3
(*R,R*)-**36i**	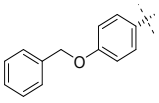	CH_3	0.118	6.7 ± 0.9
(*R,R*)-**36j**	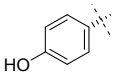	CH_3	0.120	8.4 ± 0.3

(*R,R*)-***36k***	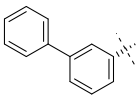	CH_3	0.100	5.6 ± 0.3
(*R,R*)-**36l**	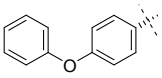	CH_3	0.085	6.9 ± 0.5
(*R,R*)-**36m**	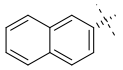	CH_3	0.103	6.6 ± 0.4
(*R,R*)-**36n**	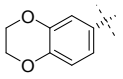	CH_3	0.078	9.5 ± 0.5
(*S,S*)-**36n**	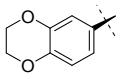	CH_3	> 10	0.7 ± 0.3

[a] Values are averages of triplicates ± SEM (2 μM PCAF, 10 μM compound).

2.3. Validation of Top Active Compounds by Biochemical Assay

In the above SAR studies, DSF and ITC assays were used to measure the bioactivity of the synthesized compounds, and a number of active compounds were identified. Because both DSF and ITC belong to biophysical assay, we then used homogeneous time-resolved fluorescence (HTRF) assay, which is a biochemical assay, to further validate the bioactivity. Here just the top active compounds were tested. As shown in Table 4, all of the tested compounds showed high potency in the HTRF assay. (*R,R*)-**36n** is again the most active one with an IC_{50} of 7 nM. For comparison, we also tested the bioactivity of ***L*-Moses**, which showed an IC_{50} of 36 nM in the HTRF assay (Figure 4B).

Table 4. Biochemical Activities (HTRF, IC_{50}) of Compounds That Showed Potent Activity in ITC and DSF Assays.

Compd	IC_{50} (μM)	Compd	IC_{50} (μM)
(*R,R*)-**24a**	0.041	(*R,R*)-**36i**	0.014

endo-**24c**	0.073	(*R,R*)-**36j**	0.030
endo-**25a**	0.125	(*R,R*)-***36k***	0.025
(*R,R*)-**36d**	0.022	(*R,R*)-**36l**	0.010
(*R,R*)-**36e**	0.032	(*R,R*)-**36m**	0.047
(*R,R*)-**36f**	0.035	(*R,R*)-**36n**	0.007
(*R,R*)-**36g**	0.017	***L*-Moses**	0.036
(*R,R*)-**36h**	0.030		

Overall, the above structural optimization and SAR studies finally led to the discovery of compound (*R,R*)-**36n**, which is among the most potent PCAF BRD inhibitors currently reported. Subsequently, further studies including selectivity profiling, interaction mode analyses, cellular activity evaluation, preliminary RNA-seq analysis, and pharmacokinetic studies were conducted on (*R,R*)-**36n**.

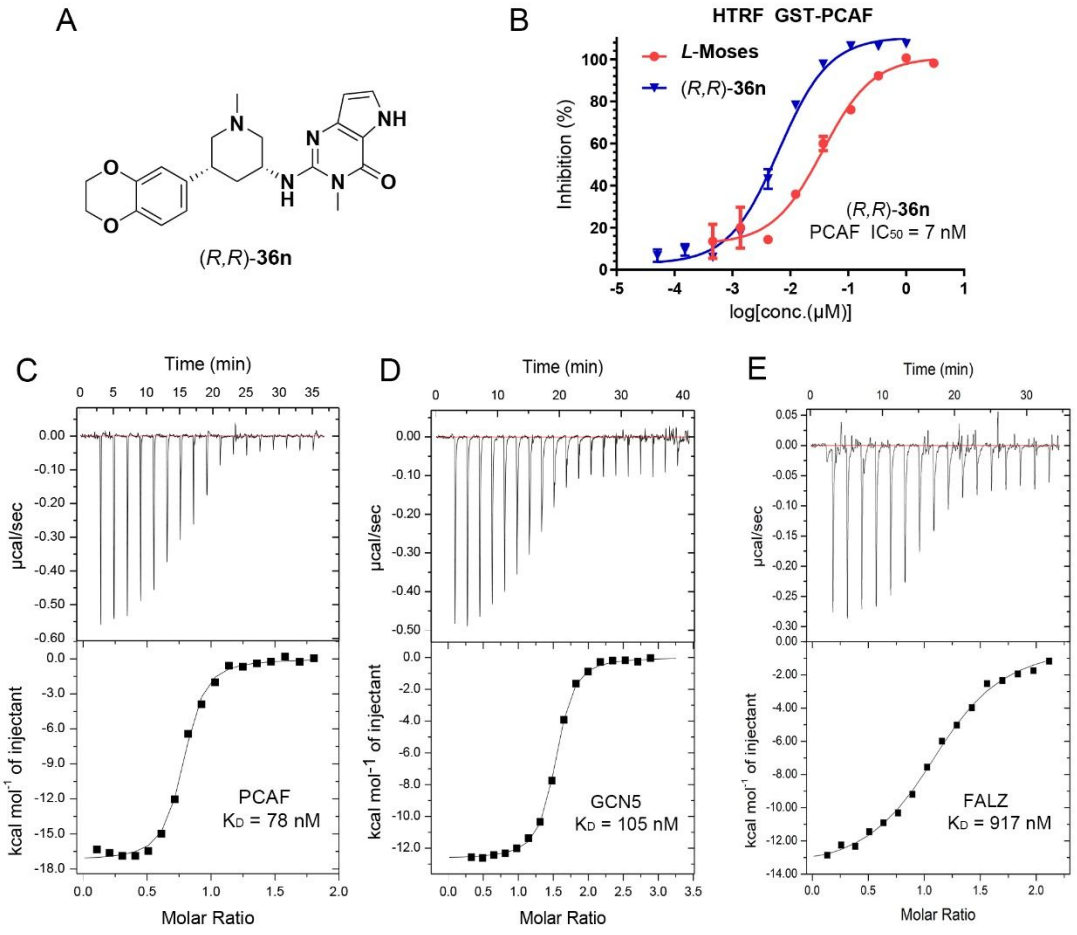

Figure 4. Identification of (*R,R*)-**36n** as a potent inhibitor of PCAF bromodomain. (A) Chemical structure of (*R,R*)-**36n**. (B) HTRF assays of (*R,R*)-**36n** and ***L*-Moses** on GST-PCAF. (C, D, E) ITC titration curves for the binding of (*R,R*)-**36n** (10 μM, 200 μL in cell) to PCAF (C, 100 μM, 40 μL in syringe), GCN5 (D, 160 μM, 40 μL in syringe) and FALZ (E, 125 μM, 40 μL in syringe).

2.4. Selectivity of (*R,R*)-36n.

To examine the selectivity of (*R,R*)-**36n**, we first used the DSF assay to measure activities of this compound against a panel of 12 BRDs available in our laboratory. (*R,R*)-**36n** showed the highest ΔT_m (9.5 °C) against PCAF. Besides PCAF, it also exhibited potent activity against GCN5 (ΔT_m = 7.3 °C) and FALZ (ΔT_m = 5.3 °C). To verify these activities, ITC was then used to determine the binding affinities of (*R,R*)-

36n against GCN5 and FALZ, which gave K_D values of 105 nM and 917 nM, respectively (Figure 4D and 4E). This is not strange because PCAF BRD, GCN5 BRD and FALZ BRD are highly homologous and share 69% sequence similarity. For the other 9 BRDs tested, (*R,R*)-**36n** displayed obviously weak or no activity (Figure 5A, Supporting Information Table S1).

Further, the commercial BROMOscan assay was used to test the activity of this compound against a panel of 32 BRDs. Consistent with the results from previous DSF assays, (*R,R*)-**36n** (1 μM) showed potent activity against PCAF, GCN5, and FALZ. It also showed activity but much weaker against CECR2, BRPF, and BAZ2 families. For the remaining 23 BRDs, (*R,R*)-**36n** did not show activity (Figure 5B, Supporting Information Table S2).

In addition, we also tested the activity of (*R,R*)-**36n** against a panel of 422 kinases by Eurofins KinaseProfiler. Here a single concentration (10 μM) of (*R,R*)-**36n** was used. The results showed that (*R,R*)-**36n** had no activity against all these kinases (see Supporting Information Table S3).

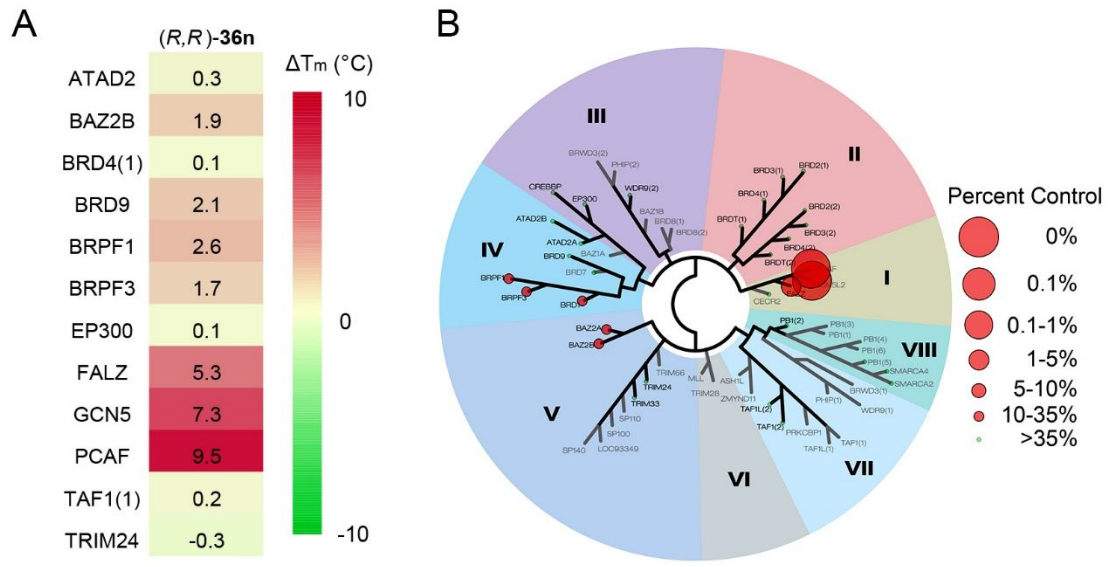

Figure 5. Selectivity of (*R,R*)-**36n**. (A) Thermal shift analysis of (*R,R*)-**36n** (10 μM)

against 12 BRDs, which belong to six distinct BRD subfamilies. The concentrations of BRDs used were 2 μM. The heat map shows the relative ΔT_m, where the red color indicates a positive ΔT_m value and the green color indicates a negative ΔT_m value. (B) DiscoverX BROMOscan bromodomain cross-screen of (*R,R*)-**36n** at 1 μM. Binding activity is expressed as a percentage of the control.

2.5. Interaction Mode of (*R,R*)-36n with its Receptor.

To understand the interaction mode of (*R,R*)-**36n** with PCAF BRD, we tried to culture the cocrystal of (*R,R*)-**36n** with PCAF BRD. Unfortunately, it was unsuccessful for some unknown reasons. We thus transferred to culture the cocrystal of (*R,R*)-**36n** bound to GCN5 BRD. As shown in Figure 6, (*R,R*)-**36n** occupies the KAc (acetylated lysine) binding site. Interactions found in the **12**-BRD complex (Figure 3A), including hydrogen bonding, π-stacking interaction, and salt bridge, all exist in the (*R,R*)-**36n**/BRD complex. Besides, we observed an additional edge-to-face aromatic interaction between the 2,3-dihydro-1,4-benzodioxine group and Trp751 in the (*R,R*)-**36n**/BRD complex, which may explain the higher activity of (*R,R*)-**36n** compared with that of **12**.

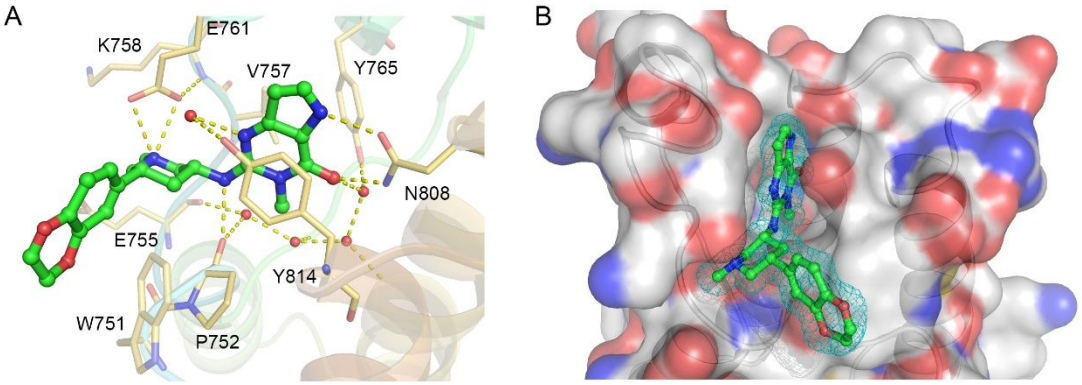

Figure 6. Structure and binding mode of (*R,R*)-**36n**. (A) X-ray cocrystal structure of (*R,R*)-**36n** (green sticks) bound to GCN5 bromodomain (PDB ID: 6J3P), with

conserved water network depicted (red spheres), yellow dashed lines indicate hydrogen bonds or salt bridges. (B) Surface view of the complex of GCN5 and (*R,R*)-**36n**. Mesh: 2Fo−Fc omitted electron density map contoured at 1.0 σ.

2.6. Bioactivity of (*R,R*)-36n in Intact Cells.

The NanoBRET assay was adopted to assess the cell permeability and target engagement potential of (*R,R*)-**36n**.[33] HEK293T cells were co-transfected with NanoLuc−tagged full-length PCAF and Halo-tagged histone H3.3 (Promega). The tagged PCAF-histone interaction in intact cells could be disrupted by competition with the test compound. In this assay, (*R,R*)-**36n** showed clear dose-dependent displacement of full length PCAF-NanoLuc from histone H3.3-HaloTag in HEK293T cells with an IC_{50} of 118 nM, indicating that (*R,R*)-**36n** could pass through the cell membrane and target PCAF, whereas the enantiomer (*S,S*)-**36n** displayed no effect (Figure 7).

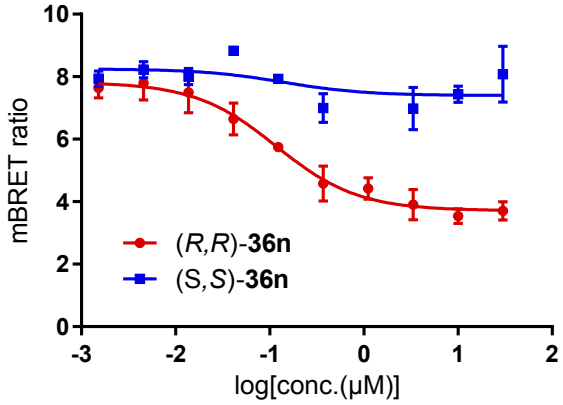

Figure 7. NanoBRET dose-response curves of (*R,R*)-**36n** and (*S,S*)-**36n** after 24 h treatment using *N*-terminal-nanoLuc-PCAF and C-terminal HaloTag-H3.3 in HEK293T cells (Graph represents n = 2 biological replicates).

2.7. Effect of (*R,R*)-36n on Global Gene Expression.

RNA-seq (RNA-sequencing) analysis was adopted to explore the effect of (*R,R*)-**36n** (2.5 μM) on global gene expression. In this assay, (*S,S*)-**36n** (2.5 μM) and DMSO were taken as negative and blank controls, respectively. Mouse embryonic fibroblast (MEF) cells were used. MEF cells were treated for 48 h in advance, and then collected for RNA-seq analysis. RNA from each set (n = 3) was used to analyze the global gene expression. As illustrated in Figure 8, treatment of (*R,R*)-**36n** significantly influenced the expression of 58 genes (> 1.5-fold), among which 49 genes (39 up-regulated and 10 down-regulated) were uniquely impacted by (*R,R*)-**36n**, which might be attributed to the role of PCAF/GCN5 BRDs. Even so, the biology significance of the gene up or down regulation needs further in-depth studies.

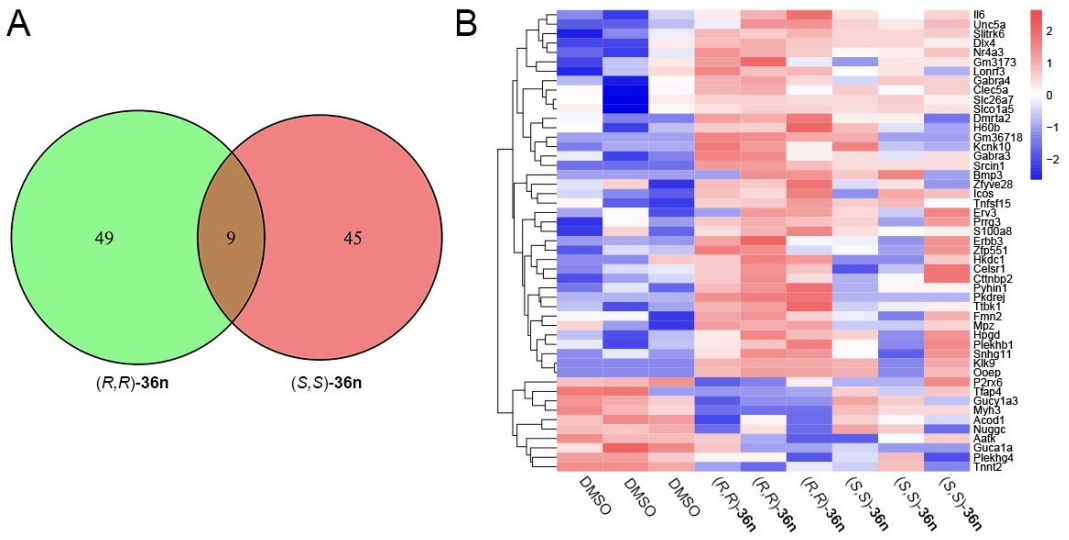

Figure 8. Effect of (*R,R*)-**36n** on global gene expression. (A) Venn diagram showing number of genes significantly up- or down-regulated greater than 1.5 fold ($p < 0.05$) following (*R,R*)-**36n**, (*S,S*)-**36n** or DMSO treatment for 48h in MEF cells. Green circle represents the number of influenced genes by (*R,R*)-**36n** relative to blank control, red circle means differential gene of (*S,S*)-**36n** relative to blank control. (B) Hierarchical

clustering heat map of selected genes showing differential regulation by (*R,R*)-**36n** and (*S,S*)-**36n** [genes up- or down-regulated by > 1.5-fold and $p < 0.05$ of (*R,R*)-**36n**]. Data from three donors are shown for each experiment.

2.8. A Preliminary Assessment for the Pharmacokinetic Properties of (*R,R*)-36n.

The pharmacokinetic characteristics of (*R,R*)-**36n** were assessed on rats. A dose of 10 mg/kg was administrated through intravenous infusion or oral administration (for the blood concentration-time profiles, see Supporting Information Figure S3). The key oral administration pharmacokinetic parameters calculated are summarized in Table 4. The area under the concentration-time curve ($AUC_{0-\infty}$) is 2486 h·ng/mL. The half-life ($T_{1/2}$) and the maximum plasma concentration (C_{max}) are 1.51 h and 1418 ng/mL, respectively. Importantly, (*R,R*)-**36n** has an excellent bioavailability of 52%. In addition, the measured *in vitro* clearance of (*R,R*)-**36n** is 45 mL/min/kg in human liver microsomes (Supporting Information Table S5). The aqueous solubility and $LogD_{pH7.4}$ measured by HPLC are 480 μM and 1.9, respectively. Because it is the unbound drug that drives efficacy according to the free drug hypothesis, we thus determined the fraction unbound (fu_b) in the Sprague-Dawley rat plasma, which gave an average value of 5.8%. All of these results indicate that (*R,R*)-**36n** possesses favorable pharmacokinetic properties.

Table 4. Key Pharmacokinetic Parameters of (*R,R*)-**36n** (p.o.).

Parameter	Value[a]
$T_{1/2}$ (h)	1.51 ± 0.23
T_{max} (h)	0.67 ± 0.29

C_{max} (ng/mL)	1418 ± 252
$AUC_{(0-t)}$ (h·ng/mL)	2479 ± 399
$AUC_{(0-\infty)}$ (h·ng/mL)	2486 ± 403
F (%)	52 ± 8.3

[a] Expressed as Mean ± SD, n = 3

3. CONCLUDING REMARKS

In this investigation, we discovered a potent PCAR BRD inhibitor, (*R,R*)-**36n**. This compound contains a new scaffold, pyrrolo[3,2-d]pyrimidin-4-one. Besides, it also contains a substituted piperidine, which is a common feature and presents in two other reported series of active compounds (**7** and **9** in Figure 1).[23, 25] In addition to the PCAF inhibition, (*R,R*)-**36n** also showed activity against GCN5 and FALZ, but displayed very weak or no activity against other 29 BRDs and 422 kinases, indicating considerable selectivity. Interestingly, the enantiomer (*S*,*S*)-**36n** did not show activity against PCAF, implying that (*R*,*R*)-**36n** could be a very suitable probe in investigating the biologic functions of PCAF. RNA-seq analysis demonstrated that (*R*,*R*)-**36n** treatment affected the expression of 49 genes on MEF cells. However, the effects of the gene expression changes on biological functions are unknown, which needs further in-depth studies. Overall, we have obtained a potent and selective PCAF inhibitor. Nevertheless, the exploring of biological functions and medicinal applications of this compound still needs intensive studies.

4. EXPERIMENTAL PROCEDURES

4.1. Chemistry. All reagents and solvents were purchased from commercial suppliers without further purification unless otherwise indicated. All reactions were monitored

by thin-layer chromatography (TLC) and visualized with UV light, ninhydrin stain, or iodine stain. Column chromatography was performed on pre-packed silica gel columns using a Biotage Isolera One flash purification system (LPLC). HPLC was performed on a Waters 2695 HPLC system. Gemini C18 reversed-phase column (4.6 mm Φ × 150 mm, 5 μm) was used for purity analysis, solubility and logD determinations and Daicel Chiralpak IE chiral column (part no. 85325; 4.6 mm Φ × 150 mm; 5 μm) for enantiomeric excess (*ee*) determination. ^{1}H NMR and ^{13}C NMR spectra were recorded on a Bruker AV-400 spectrometer. Coupling constants (J) are expressed in hertz (Hz). Chemical shifts are reported as parts per million (ppm) relative to an internal solvent reference. The following abbreviations were used in the NMR descriptions: s, singlet; d, doublet; t, triplet; q, quartet; m, multiplet; dd, double doublet; and br, broad peak. High-resolution ESI-MS data were recorded on an Agilent 1200-G6410A mass spectrometer. Purity of screening compounds were evaluated by NMR spectroscopy and HPLC analysis. All compounds had purity ≥95% by HPLC.

2-chloro-3-methyl-3H,4H,5H-pyrrolo[3,2-d]pyrimidin-4-one (**16**). *Step 1*. 2,4-dichloro-5H-pyrrolo[3,2-d]pyrimidine (**13**, 25g, 133 mmol) was added to 200 mL 1 M NaOH solution and stirred at 100 °C for 16 hours. Upon cooling to rt, the dark brown solution was acidified to pH 5 with 3 N HCl. The precipitate was collected by filtration onto a sintered-glass funnel, washed with water (2 × 50 mL), and dried in vacuo to give 2-chloro-3H,4H,5H-pyrrolo[3,2-d]pyrimidin-4-one (**14**, 20.3 g, 120 mmol, 90%) as a brown solid. ^{1}H NMR (400 MHz, DMSO-d_6) δ 12.81 (s, 1H), 12.25 (s, 1H), 7.41 (t, *J*

= 3.0 Hz, 1H), 6.35 (dd, *J* = 2.8, 2.0 Hz, 1H).

Step 2. Compound **14** (20.3 g, 120 mmol), Boc_2O (28.7 g, 132 mmol), triethylamine (13.3 g, 132 mmol), and DMAP (500 mg, 2.25 mmol) were suspended in 150 mL DMF. The mixture was stirred overnight at ambient temperature. Then 450 mL water was added and the resulting solution was acidified to pH 6 with citric acid. The precipitate was collected by filtration onto a sintered-glass funnel, washed with water (2 × 50 mL), and dried in vacuo to give *tert*-butyl 2-chloro-4-oxo-3H,4H,5H-pyrrolo[3,2-d]pyrimidine-5-carboxylate (**15**, 26.6 g, 98.6 mmol, 82%) as a brown solid. The product was used without further purification. ^{1}H NMR (400 MHz, DMSO-d_6) δ 13.07 (s, 1H), 7.85 (d, *J* = 3.5 Hz, 1H), 6.55 (d, *J* = 3.5 Hz, 1H), 1.58 (s, 9H).

Step 3. NaH (60% in mineral oil, 1.9 g, 47.5 mmol) was added portionwise to a stirred solution of **15** (8.7 g, 32.3 mmol) in anhydrous DMF (100 mL) at 0 °C. Twenty minutes later, iodomethane (6.67 g, 47 mmol) was added and the mixture was reacted at 40 °C overnight. After cooling to rt, the mixture was carefully diluted with water and extracted with ethyl acetate (EtOAc). The combined organic phase was added trifluoroacetic acid (TFA) and stirred for another 5 hours. Then the solvent was removed under reduced pressure. The residue was purified by Biotage Isolera LPLC to give **16** (2.7 g, 14.7 mmol, 46%) as a white solid. ^{1}H NMR (400 MHz, DMSO-d_6) δ 12.28 (s, 1H), 7.43 (t, *J* = 2.9 Hz, 1H), 6.35 (t, *J* = 2.2 Hz, 1H), 3.62 (s, 3H). ^{13}C NMR (101 MHz, DMSO-d6) δ 154.30, 142.50, 141.19, 129.18, 116.20, 102.98, 32.96.

***tert*-butyl (3*R*)-3-(pyridine-2-amido)piperidine-1-carboxylate ((*R*)-18a).** To a stirred solution of picolinic acid (11.1 g, 130 mmol), *tert*-butyl (3R)-3-[(pyridin-2-

yl)amido]piperidine-1-carboxylate ((*R*)-**17a**, 25.0 g, 125 mmol), and DIPEA (15.0 g, 155 mmol) in DCM (250 mL) was added HATU (50.0 g, 131.5 mmol). The mixture was stirred at ambient temperature overnight, and concentrated under reduced pressure. The residue was dissolved in EtOAc (200 mL) and washed with 0.05 M HCl (2 × 100 mL) and sat. aq $NaHCO_3$ (2 × 100 mL). The organic layer was concentrated in vacuo and purified by Biotage Isolera LPLC to give the title compound (*R*)-**18a** (32.1 g, 107 mmol, 84%) as a white solid. ^{1}H NMR (400 MHz, DMSO-d_6) δ 8.64 (dt, J = 4.7, 1.3 Hz, 1H), 8.55 (d, J = 8.2 Hz, 1H), 8.10 – 7.97 (m, 2H), 7.61 (ddd, J = 7.4, 4.8, 1.5 Hz, 1H), 3.96 – 3.43 (m, 3H), 3.26 – 2.77 (m, 2H), 1.93 – 1.79 (m, 1H), 1.79 – 1.58 (m, 2H), 1.57 – 1.20 (m, 10H). Chiral HPLC (Chiralpak IE-H column, 4.6 mm × 25 cm, 20% *i*-PrOH/hexane, 1 mL/min): R_t = 25.86 min, > 99% *ee*.

***tert*-butyl (3*R*,5*R*)-3-phenyl-5-(pyridine-2-amido)piperidine-1-carboxylate ((*R,R*)-19a).** A pressure vial (250 mL) equipped with a magnetic stirring bar was charged with compound (*R*)-**18a** (7.2 g, 23.6 mmol), iodobenzene (24.1 g, 117.89 mmol), silver carbonate (6.5 g, 23.6 mmol), palladium acetate (529 mg, 2.36 mmol), 2,6-dimethylbenzoic acid (885 mg, 5.9 mmol), and 60 mL *t*-BuOH. The vessel was flushed with argon, sealed with a crimp cap, and heated to 120 °C. After 24 h, the reaction vessel was removed from the oil bath, cooled to room temperature, and added DCM (60 mL) to the reaction mixture. The mixture was thoroughly stirred for 10 min, and the solids were removed by filtration. The filtrate was concentrated under reduced pressure and purified by Biotage Isolera LPLC to give the title compound (*R,R*)-**19a** (6.91 g, 18.1 mmol, 77%) as a white solid. ^{1}H NMR (400 MHz, DMSO-d_6) δ 8.74 –

8.62 (m, 2H), 8.10 – 7.96 (m, 2H), 7.61 (ddd, *J* = 7.4, 4.7, 1.4 Hz, 1H), 7.38 – 7.20 (m, 5H), 4.17 – 3.91 (m, 3H), 2.91 – 2.63 (m, 3H), 2.08 – 1.92 (m, 2H), 1.43 (s, 9H). Chiral HPLC (Chiralpak IE-H column, 4.6 mm × 25 cm, 20% EtOH/hexane, 1 mL/min): R_t = 31.52 min, > 99% *ee*.

(3*R*,5*R*)-1-methyl-5-phenylpiperidin-3-amine dihydrochloride ((*R,R*)-20a). *Step 1*. To a stirred solution of (*R,R*)-**19a** (6.8 g, 17.8 mmol) in DCM (80 mL) was added trifluoroacetic acid (6 mL). The resulting mixture was stirred at room temperature for 4 h. The solvent was removed under reduced pressure and the crude product was redissolved in water (60 mL). The solution was basified to pH 10 with 15% aq. NaOH and extracted twice with EtOAc. The combined organic layer was dried over anhydrous Na_2SO_4, filtered, and concentrated in vacuo to give *N*-[(3*R,*5*R*)-5-phenylpiperidin-3-yl]pyridine-2-carboxamide (4.72 g, 16.8 mmol, 94%) as a pale-yellow solid that required no further purification.

Step 2. A stirred solution of *N*-[(3*R*,5*R*)-5-phenylpiperidin-3-yl]pyridine-2-carboxamide (3.2 g, 9.03 mmol) in methanol (80 mL) was treated with glacial acetic acid (0.1 mL) and 37% w/v formaldehyde in water (1.1 mL), then with sodium triacetoxyborohydride (4.1 g, 19.33 mmol) portionwise (1.25 g every 20 min). 2 h after the final addition, the solvent was removed in vacuo and the residue was partitioned between EtOAc and water. The aqueous phase was extracted twice with EtOAc, and the combined organics were washed with brine, dried over anhydrous Na_2SO_4, filtered, and concentrated. Purification of the residue by Biotage Isolera LPLC gave *N*-[(3*R*,5*R*)-1-methyl-5-phenylpiperidin-3-yl]pyridine-2-carboxamide (2.82 g, 9.55 mmol, 84%) as

a white solid. ^{1}H NMR (400 MHz, DMSO-d_6) δ 8.64 (dt, J = 4.8, 1.3 Hz, 1H), 8.56 (d, J = 8.7 Hz, 1H), 8.08 – 7.95 (m, 2H), 7.60 (ddd, J = 7.3, 4.7, 1.5 Hz, 1H), 7.36 – 7.25 (m, 4H), 7.25 – 7.16 (m, 1H), 4.20 – 4.06 (m, 1H), 2.98 – 2.80 (m, 3H), 2.24 (s, 3H), 2.01 – 1.84 (m, 3H), 1.75 (q, J = 12.2 Hz, 1H).

Step 3. To a suspension of *N*-[(3*R*,5*R*)-1-methyl-5-phenylpiperidin-3-yl]pyridine-2-carboxamide (2.8 g, 9.48 mmol) in *i*-PrOH (80 mL) was added NaOH (3.8 g, 95 mmol). The mixture was stirred at 85 °C for 18 h. Then the solvent was removed under reduced pressure and water (50 mL) was added. The solution was extracted with EtOAc (50 mL × 2). The combined organic layer was dried over anhydrous Na_2SO_4, filtered, and added 15% HCl in ethanol (1 mL). Finally the solvent was removed in vacuo to give (*R,R*)-**20a** (2.11 g, 85%, 8.0 mmol) as a pale-white solid. ^{1}H NMR (400 MHz, DMSO-d_6) δ 11.78 (s, 1H), 8.80 (s, 3H), 7.44 – 7.21 (m, 5H), 3.81 – 3.70 (m, 1H), 3.64 – 3.56 (m, 1H), 3.54 – 3.46 (m, 1H), 3.37 – 3.26 (m, 1H), 3.25 – 3.05 (m, 2H), 2.84 (s, 3H), 2.28 (d, J = 12.3 Hz, 1H), 1.82 (q, J = 12.3 Hz, 1H).

3-methyl-2-{[(3*R*,5*R*)-1-methyl-5-phenylpiperidin-3-yl]amino}-3H,4H,5H-pyrrolo[3,2-d]pyrimidin-4-one ((*R,R*)-24a). A solution of **16** (200 mg, 1.09 mmol) in NMP was treated with (*R,R*)-**20a** (344 mg, 1.31 mmol) and DIPEA (183 mg, 1.42 mmol). Then the reaction was heated to 150 °C and stirred at this temperature for 2 h. After cooling to ambient temperature, the mixture was diluted with EtOAc and water. The biphasic solution was extracted twice with EtOAc. The combined organics were washed with brine, dried over anhydrous $MgSO_4$, and concentrated in vacuo. Purification of the residue by Biotage Isolera LPLC gave the title compound (*R,R*)-**24a**

(53 mg, 0.157 mmol, 14%) as a white solid. ^{1}H NMR (400 MHz, DMSO-d_6) δ 11.37 (s, 1H), 7.36 – 7.13 (m, 5H), 7.11 (t, J = 2.9 Hz, 1H), 6.01 (t, J = 2.5 Hz, 1H), 5.97 (d, J = 7.7 Hz, 1H), 4.22 – 4.10 (m, 1H) , 3.31 (s, 3H), 3.07 (dd, J = 10.4, 4.1 Hz, 1H), 2.92 – 2.78 (m, 2H), 2.20 (s, 3H), 2.04 (dd, J = 12.0, 4.2 Hz, 1H), 1.91 – 1.75 (m, 2H), 1.57 (q, J = 12.1 Hz, 1H). ^{13}C NMR (101 MHz, DMSO-d_6) δ 154.48, 149.57, 144.80, 143.97, 128.88, 127.80, 127.47, 126.86, 112.40, 101.18, 62.49, 60.33, 48.62, 46.14, 41.62, 37.11, 27.72. HRMS *m*/*z* 338.1985 (M + H$^+$, $C_{21}H_{25}N_5O_3$, requires 337.1903). Chiral HPLC (Chiralpak IE-H column, 4.6 mm × 25 cm, 25% *i*-PrOH/hexane, 1 mL/min): R_t = 16.53 min, > 99% *ee*.

3-methyl-2-{[(3*S*,5*S*)-1-methyl-5-phenylpiperidin-3-yl]amino}-3H,4H,5H-pyrrolo[3,2-d]pyrimidin-4-one ((*S,S*)-24a). The title compound (*S,S*)-**24a** was prepared in the same manner as shown for (*R,R*)-**24a** except *tert*-butyl (3S)-3-aminopiperidine-1-carboxylate (*S*)-**17a** was used instead. ^{1}H NMR (400 MHz, DMSO-d_6) δ 11.42 (s, 1H), 7.36 – 7.19 (m, 5H), 7.15 (t, J = 2.9 Hz, 1H), 6.05 (t, J = 2.5 Hz, 1H), 6.00 (d, J = 7.7 Hz, 1H), 4.26 – 4.13 (m, 1H), 3.36 (s, 3H), 3.10 (dd, J = 10.4, 4.2 Hz, 1H), 2.95 – 2.82 (m, 2H), 2.23 (s, 3H), 2.11 – 2.04 (m, 1H), 1.93 – 1.76 (m, 2H), 1.62 (q, J = 12.1 Hz, 1H). ^{13}C NMR (101 MHz, DMSO-d_6) δ 154.47, 149.57, 144.80, 144.06, 128.88, 127.77, 127.47, 126.84, 112.40, 101.18, 62.63, 60.46, 48.68, 46.23, 41.70, 37.16, 27.71. HRMS *m*/*z* 338.1987 (M + H$^+$, $C_{19}H_{23}N_5O$, requires 337.1903). Chiral HPLC (Chiralpak IE-H column, 4.6 mm × 25 cm, 25% *i*-PrOH/hexane, 1 mL/min): R_t = 14.23 min, > 99% *ee*.

3-methyl-2-[(*cis*-1-methyl-6-phenylazepan-4-yl)amino]-3H,4H,5H-pyrrolo[3,2-d]pyrimidin-4-one (*cis*-24b). The title compound *cis*-**24b** was prepared in the same manner as shown for (*R,R*)-**24a** except *tert*-butyl 4-aminoazepane-1-carboxylate **17b** was used instead. ^{1}H NMR (400 MHz, DMSO-d_6) δ 11.39 (s, 1H), 7.31 – 7.22 (m, 4H), 7.19 – 7.10 (m, 2H), 6.06 (d, J = 7.6 Hz, 1H), 6.02 (t, J = 2.4 Hz, 1H), 4.33 – 4.20 (m, 1H), 3.35 (s, 3H), 3.06 – 2.95 (m, 1H), 2.73 – 2.62 (m, 4H), 2.32 (s, 3H), 2.17 – 1.97 (m, 3H), 1.90 – 1.77 (m, 1H). ^{13}C NMR (101 MHz, DMSO-d_6) δ 154.52, 149.35, 147.02, 144.93, 128.83, 127.65, 127.29, 126.40, 112.31, 101.21, 65.54, 53.85, 51.10, 47.36, 43.07, 42.07, 34.76, 27.62. HRMS *m*/*z* 352.2137 (M + H$^+$, $C_{20}H_{25}N_5O$, requires 351.2059).

3-methyl-2-{[(1*R*,3*r*,5*S*)-9-methyl-9-azabicyclo[3.3.1]nonan-3-yl]amino}-3H,4H,5H-pyrrolo[3,2-d]pyrimidin-4-one (***endo*-24c**). Compound **16** (100 mg, 0.54 mmol), (1*R*,3*r*,5*S*)-9-methyl-9-azabicyclo[3.3.1]nonan-3-amine (100 mg, 0.65 mmol), and DIPEA (100 mg) were added to 4 mL NMP. The suspension was reacted at 150 °C for 2 hours. After cooling to ambient temperature, the mixture was diluted with EtOAc and water. The resulting solution was extracted twice with EtOAc. The combined organic layer was concentrated and purified by Biotage Isolera LPLC to give *endo*-**24c** (37 mg, 12.3 mmol, 22.5%) as a white solid. ^{1}H NMR (400 MHz, DMSO-d_6) δ 11.36 (s, 1H), 7.13 (t, J = 2.9 Hz, 1H), 6.03 (t, J = 2.4 Hz, 1H), 5.84 (d, J = 8.5 Hz, 1H), 4.39 (dtd, J = 14.4, 12.0, 6.5 Hz, 1H), 3.36 (s, 3H), 2.97 (d, J = 11.1 Hz, 2H), 2.41 (s, 3H), 2.29 (td, J = 12.1, 6.2 Hz, 2H), 2.18 – 2.03 (m, 1H), 1.92 (tt, J = 13.4, 4.3 Hz, 2H), 1.49 – 1.37 (m, 3H), 0.90 (d, J = 12.7 Hz, 2H). ^{13}C NMR (101 MHz, DMSO-d_6) δ 154.51,

149.78, 145.10, 127.68, 112.22, 101.06, 51.22, 43.31, 32.88, 27.67, 23.60, 14.54. HRMS *m*/*z* 302.1981 (M + H^+, $C_{16}H_{23}N_5O$, requires 301.1903).

2-{[(1*R*,3*R*,5*S*)-8-benzyl-8-azabicyclo[3.2.1]octan-3-yl]amino}-3-methyl-3H,4H,5H-pyrrolo[3,2-d]pyrimidin-4-one (*endo*-24d). The title compound *endo*-**24d** was prepared in the same manner as shown for *endo*-**24c** except commercial (1*R*,3*R*,5*S*)-8-benzyl-8-azabicyclo[3.2.1]octan-3-amine was used instead. ^{1}H NMR (400 MHz, DMSO-d_6) δ 11.46 (s, 1H), 7.42 – 7.20 (m, 5H), 7.16 (t, *J* = 2.9 Hz, 1H), 6.06 (t, *J* = 2.4 Hz, 1H), 5.56 (d, *J* = 2.9 Hz, 1H), 4.03 (t, *J* = 6.6 Hz, 1H), 3.53 (s, 2H), 3.42 (s, 3H), 3.12 (s, 2H), 2.09 – 1.94 (m, 6H), 1.89 – 1.80 (m, 2H). ^{13}C NMR (101 MHz, DMSO-d_6) δ 154.66, 149.61, 144.53, 128.81, 128.57, 127.63, 127.09, 112.84, 101.47, 58.15, 56.06, 43.69, 35.83, 27.76, 26.40. HRMS *m*/*z* 364.2139 (M + H^+, $C_{21}H_{25}N_5O$, requires 363.2059).

3-methyl-2-{[(1*R*,3*r*,5*S*)-9-azabicyclo[3.3.1]nonan-3-yl]amino}-3H,4H,5H-pyrrolo[3,2-d]pyrimidin-4-one (*endo*-25a) and 3-methyl-2-{[(1*R*,3*s*,5*S*)-9-azabicyclo[3.3.1]nonan-3-yl]amino}-3H,4H,5H-pyrrolo[3,2-d]pyrimidin-4-one (*exo*-25a). *Step 1*. *Endo*-**24e** and *exo*-**24e** were prepared in the same manner as shown for *endo*-**24c** except commercial *tert*-butyl 3-amino-9-azabicyclo[3.3.1]nonane-9-carboxylate (*endo* : *exo* = 2 : 3; 3.14 g, 131 mmol) was used instead. The crude products were purified by Biotage Isolera LPLC to give *endo*-**24e** (830 mg, 2.14 mmol) and *exo*-**24e** (1.2 g, 3.1 mmol) as white solids. *endo*-**24e**: ^{1}H NMR (400 MHz, DMSO-d_6) δ 11.39 (s, 1H), 7.14 (t, *J* = 2.9 Hz, 1H), 6.03 – 5.91 (m, 2H), 4.34 (dd, *J* = 20.2, 11.5 Hz, 2H), 3.90 – 3.79 (m, 1H), 3.35 (s, 3H), 2.37 – 2.00 (m, 4H), 1.57 – 1.33 (m, 15H).

HRMS *m*/*z* 388.2281 (M + H^+, $C_{21}H_{25}N_5O_3$, requires 387.2270). Chiral HPLC (Chiralpak IE-H column, 4.6 mm × 25 cm, 20% *i*-PrOH/hexane, 1 mL/min): R_t = 17.14 min, > 99% *ee*. *exo*-**24e**: ^{1}H NMR (400 MHz, DMSO-d_6) δ 11.40 (s, 1H), 7.14 (t, *J* = 2.9 Hz, 1H), 6.01 (t, *J* = 2.4 Hz, 1H), 5.86 (d, *J* = 7.9 Hz, 1H), 4.97 – 4.84 (m, 1H), 4.23 (d, *J* = 16.3 Hz, 2H), 3.33 (s, 3H), 2.06 – 1.86 (m, 3H), 1.75 – 1.62 (m, 6H), 1.42 (s, 9H). ^{13}C NMR (101 MHz, DMSO-d_6) δ 154.47, 153.38, 149.62, 144.85, 127.70, 112.34, 101.27, 78.78, 47.68, 46.08, 44.96, 36.78, 36.36, 29.44, 28.69, 27.68. HRMS *m*/*z* 388.2237 (M + H^+, $C_{21}H_{25}N_5O_3$, requires 387.2270). Chiral HPLC (Chiralpak IE-H column, 4.6 mm × 25 cm, 20% *i*-PrOH/hexane, 1 mL/min): R_t = 14.37 min, > 99% *ee*.

Step 2. To a stirred solution of *endo*-**24e** in DCM at room temperature was added trifluoroacetic acid. After reaction completion, the solvent was removed under reduced pressure and the residue was basified and purified to give *endo*-**25a** as white solid. *endo*-**25a**: ^{1}H NMR (400 MHz, DMSO-d_6) δ 11.41 (s, 1H), 7.15 (d, *J* = 2.8 Hz, 1H), 6.02 (d, *J* = 2.8 Hz, 1H), 5.84 (d, *J* = 8.2 Hz, 1H), 4.28 – 4.12 (m, 1H), 3.37 (s, 3H), 3.29 – 3.23 (m, 2H), 2.19 (td, *J* = 11.7, 5.9 Hz, 2H), 2.10 – 1.97 (m, 1H), 1.56 (tt, *J* = 12.8, 4.2 Hz, 2H), 1.50 – 1.41 (m, 1H), 1.39 – 1.25 (m, 4H). ^{13}C NMR (101 MHz, DMSO-d_6) δ 154.51, 149.66, 145.00, 127.69, 112.30, 101.02, 45.23, 43.68, 32.69, 32.23, 27.70, 14.54. HRMS *m*/*z* 288.1827 (M + H^+, $C_{21}H_{25}N_5O_3$, requires 287.1746). *exo*-**25a** was prepared from *exo*-**24e** using the procedure described for compound *endo*-**25a** as a white solid. *exo*-**25a**: ^{1}H NMR (400 MHz, DMSO-d_6) δ 11.40 (s, 1H), 7.14 (d, *J* = 2.8 Hz, 1H), 6.00 (d, *J* = 2.8 Hz, 1H), 5.81 (d, *J* = 7.7 Hz, 1H), 4.82 (tq, *J* = 12.2, 6.4 Hz, 1H), 3.35 (s, 3H), 3.18 – 3.13 (m, 2H), 2.05 – 1.86 (m, 3H), 1.85 – 1.60 (m,

7H). ^{13}C NMR (101 MHz, DMSO-d_6) δ 154.52, 149.66, 144.96, 127.67, 112.31, 101.24, 47.31, 45.40, 38.01, 30.43, 27.67, 21.03. HRMS *m*/*z* 288.1819 (M + H^+, $C_{21}H_{25}N_5O_3$, requires 287.1746).

3-methyl-2-{[(1*R*,3*r*,5*S*)-9-[(2*R*)-2-hydroxy-2-phenylethyl]-9-azabicyclo[3.3.1]nonan-3-yl]amino}-3H,4H,5H-pyrrolo[3,2-d]pyrimidin-4-one (*endo*-26a). To a stirred solution of *endo*-**25a** (100 mg, 0.35 mmol) and triethylamine (61 mg, 0.6 mmol) in MeCN was added (*R*)-2-phenyloxirane (60 mg, 0.5 mmol). The mixture was reacted at 70 °C overnight. After cooling to room temperature, the mixture was concentrated under reduced pressure and the residue was purified by Biotage Isolera LPLC to give *endo*-**26a** in 58% yield as a white solid. ^{1}H NMR (400 MHz, DMSO-d_6) δ 11.38 (s, 1H), 7.44 – 7.29 (m, 4H), 7.27 – 7.20 (m, 1H), 7.15 (t, *J* = 2.9 Hz, 1H), 6.05 (t, *J* = 2.4 Hz, 1H), 5.81 (d, *J* = 8.3 Hz, 1H), 4.89 (s, 1H), 4.57 (dd, *J* = 7.8, 5.1 Hz, 1H), 4.42 – 4.27 (m, 1H), 3.37 (s, 3H), 3.14 – 2.96 (m, 2H), 2.79 (dd, *J* = 13.1, 5.1 Hz, 1H), 2.68 (dd, *J* = 13.0, 7.8 Hz, 1H), 2.40 – 2.19 (m, 2H), 2.16 – 2.00 (m, 1H), 1.89 – 1.63 (m, 2H), 1.49 – 1.31 (m, 3H), 1.08 – 0.94 (m, 2H). ^{13}C NMR (101 MHz, DMSO-d_6) δ 154.53, 149.73, 145.05, 128.24, 127.73, 127.14, 126.57, 112.28, 101.11, 71.39, 61.31, 51.48, 49.95, 43.34, 32.34, 27.71, 26.78, 26.33, 14.22. HRMS *m*/*z* 408.2405 (M + H^+, $C_{23}H_{29}N_5O_2$, requires 407.2321).

3-methyl-2-{[(1*R*,3*r*,5*S*)-9-[(2*S*)-2-hydroxy-2-(pyridin-2-yl)ethyl]-9-azabicyclo[3.3.1]nonan-3-yl]amino}-3H,4H,5H-pyrrolo[3,2-d]pyrimidin-4-one (*endo*-26b). The title compound was prepared from *endo*-**25a** (100 mg, 0.75 mmol) and (*R*)-2-bromo-1-(pyridin-2-yl)ethan-1-ol (162 mg, 0.8 mmol) using the procedure

described for compound *endo*-**26a** in 47% yield as a white solid. ^{1}H NMR (400 MHz, DMSO-d_6) δ 11.38 (s, 1H), 8.57 – 8.43 (m, 1H), 7.79 (td, J = 7.7, 1.9 Hz, 1H), 7.53 (d, J = 7.8 Hz, 1H), 7.25 (dd, J = 7.4, 4.9 Hz, 1H), 7.15 (t, J = 2.9 Hz, 1H), 6.07 (t, J = 2.4 Hz, 1H), 5.80 (d, J = 8.3 Hz, 1H), 5.10 (s, 1H), 4.62 (dd, J = 7.9, 4.1 Hz, 1H), 4.39 – 4.26 (m, 1H), 3.37 (s, 3H), 3.13 – 2.96 (m, 3H), 2.70 (dd, J = 13.1, 7.9 Hz, 1H), 2.29 (dp, J = 16.2, 5.1 Hz, 2H), 2.15 – 2.01 (m, 1H), 1.86 – 1.67 (m, 2H), 1.47 – 1.33 (m, 3H), 1.00 (d, J = 12.8 Hz, 2H). ^{13}C NMR (101 MHz, DMSO-d_6) δ 163.80, 154.53, 149.72, 148.66, 145.03, 136.80, 127.73, 122.45, 121.03, 112.26, 101.12, 72.86, 59.56, 51.48, 49.98, 43.31, 32.38, 27.71, 26.71, 26.28, 14.22. HRMS *m*/*z* 409.2359 (M + H$^+$, $C_{22}H_{28}N_6O_2$, requires 408.2274).

2-chloro-3-ethyl-3H,4H,5H-pyrrolo[3,2-d]pyrimidin-4-one (27a). **27a** was prepared from **15** (2.0 g, 7.42 mmol) and iodoethane (1.5 g, 9.65 mmol) using the procedure described for **16** in 51% yield as a white solid. ^{1}H NMR (400 MHz, DMSO-d_6) δ 12.29 (s, 1H), 7.43 (t, J = 2.9 Hz, 1H), 6.35 (dd, J = 2.9, 2.0 Hz, 1H), 4.24 (q, J = 7.1 Hz, 2H), 1.26 (t, J = 7.1 Hz, 3H).

2-chloro-3-(prop-2-en-1-yl)-3H,4H,5H-pyrrolo[3,2-d]pyrimidin-4-one (27b). **27b** was prepared from **15** (2.0 g, 7.42 mmol) and 3-bromoprop-1-ene (1.17 g, 9.65 mmol) using the procedure described for **16** in 49% yield as a white solid. ^{1}H NMR (400 MHz, DMSO-d_6) δ 12.33 (s, 1H), 7.46 (t, J = 2.9 Hz, 1H), 6.38 (t, J = 2.4 Hz, 1H), 6.02 – 5.90 (m, 1H), 5.20 (dq, J = 10.5, 1.6 Hz, 1H), 5.02 (dq, J = 17.1, 1.7 Hz, 1H), 4.83 (dt, J = 4.9, 1.8 Hz, 2H).

3-(but-3-en-1-yl)-2-chloro-3H,4H,5H-pyrrolo[3,2-d]pyrimidin-4-one (27c). **27c** was prepared from **15** (2.0 g, 7.42 mmol) and 4-bromobut-1-ene (1.30 g, 9.65 mmol) using the procedure described for **16** in 34% yield as a white solid. ^{1}H NMR (400 MHz, DMSO-d_6) δ 12.29 (s, 1H), 7.44 (t, J = 2.9 Hz, 1H), 6.35 (dd, J = 2.9, 2.0 Hz, 1H), 5.90 – 5.80 (m, 1H), 5.09 – 5.00 (m, 2H), 4.32 – 4.22 (m, 2H), 2.45 (q, J = 7.1 Hz, 2H).

3-(but-2-en-1-yl)-2-chloro-3H,4H,5H-pyrrolo[3,2-d]pyrimidin-4-one (27d). **27d** was prepared from **15** (2.0 g, 7.42 mmol) and 1-bromobut-2-ene (1.30 g, 9.65 mmol) using the procedure described for **16** in 39% yield as a white solid. ^{1}H NMR (400 MHz, DMSO-d_6) δ 12.31 (s, 1H), 7.45 (t, J = 3.0 Hz, 1H), 6.36 (dd, J = 2.8, 2.0 Hz, 1H), 5.64 – 5.52 (m, 2H), 4.81 – 4.70 (m, 2H), 1.80 – 1.72 (m, 1H), 1.68 – 1.62 (m, 2H).

2-chloro-3,5-dimethyl-3H,4H,5H-pyrrolo[3,2-d]pyrimidin-4-one (**28**). NaH (60% in mineral oil, 400 mg, 10.0 mmol) was added portionwise to a stirred solution of **14** (1.2 g, 7.08 mmol) in anhydrous DMF (30 mL) at 0 °C. Twenty minutes later, iodomethane (2.27 g, 16.0 mmol) was added. The mixture was reacted at 60 °C for 5 h. After cooling to rt, the reaction mixture was diluted with water and extracted with EtOAc. The combined organic phase was concentrated under reduced pressure and the residue was purified by Biotage Isolera LPLC (PE/EA 10:1- 2:1) to give **28** (1.09 g, 78%) as a white solid. ^{1}H NMR (400 MHz, DMSO-d_6) δ 7.43 (d, J = 2.9 Hz, 1H), 6.30 (d, J = 2.9 Hz, 1H), 3.98 (s, 3H), 3.58 (s, 3H).

2-chloro-3-methyl-3H,4H-thieno[3,2-d]pyrimidin-4-one (31). *Step 1.* 2-chloro-3H,4H-thieno[3,2-d]pyrimidin-4-one **30** (1.73 g, 9.27 mmol, 95%) was prepared from **29** (2.0 g, 9.75 mmol) using the procedure described for **14** as a yellow solid.

Step 2. **31** (1.43 g, 77%) was prepared from **30** (1.73 g, 9.27 mmol) and iodomethane (1.8 g, 12.7 mmol) using the procedure described for **28** as a yellow solid. ^{1}H NMR (400 MHz, DMSO-d_6) δ 8.24 (d, J = 5.2 Hz, 1H), 7.37 (d, J = 5.2 Hz, 1H), 3.64 (s, 3H).

3-ethyl-2-{[(3*R*,5*R*)-1-methyl-5-phenylpiperidin-3-yl]amino}-3H,4H,5H-pyrrolo[3,2-d]pyrimidin-4-one ((*R,R*)-32a). The title compound was prepared from **27a** (180 mg, 0.91 mmol) and (*R,R*)-**20a** (264 mg, 1.0 mmol) using the procedure described for compound (*R,R*)-**24a** in 13% yield as a white solid. ^{1}H NMR (400 MHz, DMSO-d_6) δ 11.40 (s, 1H), 7.36 – 7.19 (m, 5H), 7.15 (t, J = 2.9 Hz, 1H), 6.09 – 6.01 (m, 2H), 4.25 (dtt, J = 11.5, 7.5, 4.0 Hz, 1H), 4.07 (q, J = 7.0 Hz, 2H), 3.09 (dd, J = 10.5, 4.1 Hz, 1H), 2.96 – 2.83 (m, 2H), 2.24 (s, 3H), 2.03 (dd, J = 10.0, 6.1 Hz, 1H), 1.94 – 1.77 (m, 2H), 1.65 (q, J = 12.1 Hz, 1H), 1.12 (t, J = 7.0 Hz, 3H). ^{13}C NMR (101 MHz, DMSO-d_6) δ 154.30, 148.65, 144.82, 144.09, 128.87, 127.77, 127.48, 126.84, 112.57, 101.13, 62.53, 60.43, 48.56, 46.22, 41.75, 37.19, 34.90, 13.73. HRMS *m*/*z* 352.2136 (M + H$^+$, $C_{20}H_{25}N_5O$, requires 351.2059).

2-{[(3*R*,5*R*)-1-methyl-5-phenylpiperidin-3-yl]amino}-3-(prop-2-en-1-yl)-3H,4H,5H-pyrrolo[3,2-d]pyrimidin-4-one ((*R,R*)-32b). The title compound was prepared from **27b** (190 mg, 0.91 mmol) and (*R,R*)-**20a** (264 mg, 1.0 mmol) using the procedure described for compound (*R,R*)-**24a** in 17% yield as a white solid. ^{1}H NMR (400 MHz, DMSO-d_6) δ 11.46 (s, 1H), 7.34 – 7.16 (m, 6H), 6.06 (t, J = 2.4 Hz, 1H), 5.91 – 5.80 (m, 1H), 5.76 (d, J = 7.8 Hz, 1H), 5.12 – 5.05 (m, 1H), 5.01 – 4.93 (m, 1H), 4.71 (d, J = 4.8 Hz, 2H), 4.21 (dd, J = 7.2, 3.7 Hz, 1H), 3.06 (dd, J = 10.6, 4.3 Hz, 1H),

2.95 – 2.81 (m, 2H), 2.23 (s, 3H), 2.01 (d, J = 12.3 Hz, 1H), 1.89 (t, J = 10.8 Hz, 1H), 1.76 (t, J = 10.5 Hz, 1H), 1.56 (q, J = 12.1 Hz, 1H). ^{13}C NMR (101 MHz, DMSO-d_6) δ 154.19, 148.76, 144.99, 144.04, 133.40, 128.87, 128.01, 127.47, 126.84, 115.94, 112.31, 101.25, 62.45, 60.39, 48.62, 46.20, 46.17, 41.68, 41.52, 37.29. HRMS *m*/*z* 364.2133 (M + H$^+$, $C_{21}H_{25}N_5O$, requires 363.2059).

3-(but-3-en-1-yl)-2-{[(3*R*,5*R*)-1-methyl-5-phenylpiperidin-3-yl]amino}-3H,4H,5H-pyrrolo[3,2-d]pyrimidin-4-one ((*R*,*R*)-32c). The title compound was prepared from **27c** (180 mg, 0.8 mmol) and (*R,R*)-**20a** (233 mg, 0.88 mmol) using the procedure described for compound (*R*,*R*)-**24a** in 19% yield as a white solid. ^{1}H NMR (400 MHz, DMSO-d_6) δ 11.38 (s, 1H), 7.36 – 7.26 (m, 4H), 7.26 – 7.18 (m, 1H), 7.15 (t, J = 2.9 Hz, 1H), 6.08 – 5.99 (m, 2H), 5.82 (ddt, J = 17.0, 10.2, 6.7 Hz, 1H), 5.05 – 4.93 (m, 2H), 4.24 (td, J = 11.4, 9.4, 5.2 Hz, 1H), 4.13 (dd, J = 8.4, 6.3 Hz, 2H), 3.12 – 3.04 (m, 1H), 2.97 – 2.79 (m, 2H), 2.32 (q, J = 7.1 Hz, 2H), 2.24 (s, 3H), 2.04 (dd, J = 10.0, 6.1 Hz, 1H), 1.93 – 1.78 (m, 2H), 1.63 (q, J = 12.1 Hz, 1H). ^{13}C NMR (101 MHz, DMSO-d_6) δ 154.49, 148.74, 144.76, 144.09, 135.68, 128.88, 127.81, 127.48, 126.84, 117.24, 112.52, 101.17, 62.50, 60.39, 48.63, 46.22, 41.75, 38.76, 37.23, 32.27. HRMS *m*/*z* 378.2293 (M + H$^+$, $C_{22}H_{27}N_5O$, requires 377.2216).

3-[(2*E*/*Z*)-but-2-en-1-yl]-2-{[(3*R*,5*R*)-1-methyl-5-phenylpiperidin-3-yl]amino}-3H,4H,5H-pyrrolo[3,2-d]pyrimidin-4-one ((*R*,*R*)-32d). The title compound was prepared from **27d** (180 mg, 0.8 mmol) and (*R,R*)-**20a** (233 mg, 0.88 mmol) using the procedure described for compound (*R,R*)-**24a** in 14% yield as a white solid. ^{1}H NMR (400 MHz, DMSO-d_6) δ 11.42 (s, 1H), 7.36 – 7.19 (m, 5H), 7.16 (t, J =

2.9 Hz, 1H), 6.05 (t, *J* = 2.4 Hz, 1H), 5.76 (d, *J* = 7.8 Hz, 1H), 5.59 – 5.40 (m, 2H), 4.62 (d, *J* = 4.9 Hz, 2H), 4.24 – 4.12 (m, 1H), 3.06 (dd, 1H), 2.93 – 2.82 (m, 2H), 2.24 (s, 3H), 2.02 (dt, *J* = 12.4, 3.9 Hz, 1H), 1.95 – 1.87 (m, 1H), 1.76 (t, 1H), 1.65 – 1.50 (m, 4H). ^{13}C NMR (101 MHz, DMSO-d_6) δ 154.20, 148.77, 144.87, 144.02, 128.89, 127.94, 127.69, 127.48, 126.86, 125.86, 112.44, 101.20, 62.43, 60.40, 48.61, 46.18, 41.65, 40.82, 37.25, 17.86. HRMS *m*/*z* 378.2295 (M + H$^+$, $C_{22}H_{27}N_5O$, requires 377.2216).

3,5-dimethyl-2-{[(3*R*,5*R*)-1-methyl-5-phenylpiperidin-3-yl]amino}-3H,4H,5H-pyrrolo[3,2-d]pyrimidin-4-one ((*R,R*)-32e). The title compound was prepared from **28** (150 mg, 0.76 mmol) and (*R,R*)-**20a** (224 mg, 0.85 mmol) using the procedure described for compound (*R,R*)-**24a** in 23% yield as a white solid. ^{1}H NMR (400 MHz, DMSO-d_6) δ 7.36 – 7.19 (m, 5H), 7.15 (d, *J* = 2.8 Hz, 1H), 6.03 (d, *J* = 7.8 Hz, 1H), 5.99 (d, *J* = 2.8 Hz, 1H), 4.24 – 4.13 (m, 1H), 3.88 (s, 3H), 3.33 (s, 3H), 3.09 (dd, *J* = 10.4, 4.1 Hz, 1H), 2.97 – 2.80 (m, 2H), 2.23 (s, 3H), 2.07 (dd, *J* = 11.5, 4.2 Hz, 1H), 1.85 (dt, *J* = 27.9, 10.6 Hz, 2H), 1.62 (q, *J* = 12.1 Hz, 1H). ^{13}C NMR (101 MHz, DMSO-d_6) δ 154.90, 149.66, 145.21, 144.04, 132.37, 128.87, 127.47, 126.84, 112.17, 100.02, 62.60, 60.42, 48.62, 46.21, 41.68, 37.13, 35.56, 27.45. HRMS *m*/*z* 352.2136 (M + H$^+$, $C_{20}H_{25}N_5O$, requires 351.2059).

3-methyl-2-{[(3*R*,5*R*)-1-methyl-5-phenylpiperidin-3-yl]amino}-3H,4H-thieno[3,2-d]pyrimidin-4-one ((*R,R*)-32f). The title compound was prepared from **31** (150 mg, 0.75 mmol) and (*R,R*)-**20a** (211 mg, 0.8 mmol) using the procedure described for compound (*R,R*)-**24a** in 47% yield as a white solid. ^{1}H NMR (400 MHz, DMSO-d_6) δ 7.96 (d, *J* = 5.3 Hz, 1H), 7.38 – 7.26 (m, 4H), 7.25 – 7.20 (m, 1H), 7.10 (d, *J* = 5.3

Hz, 1H), 6.60 (d, *J* = 7.9 Hz, 1H), 4.30 (ddd, *J* = 18.5, 9.7, 6.3 Hz, 1H), 3.40 (s, 3H), 3.08 (dd, *J* = 10.5, 4.2 Hz, 1H), 2.98 – 2.81 (m, 2H), 2.24 (s, 3H), 2.07 (dt, *J* = 12.1, 3.8 Hz, 1H), 1.88 (q, *J* = 10.6 Hz, 2H), 1.69 (q, *J* = 12.1 Hz, 1H). ^{13}C NMR (101 MHz, DMSO-d_6) δ 158.20, 157.96, 152.92, 143.91, 134.95, 128.88, 127.46, 126.87, 124.49, 112.10, 62.48, 60.12, 48.90, 46.18, 41.63, 36.89, 28.16. HRMS *m*/*z* 355.1560 (M + H$^+$, $C_{19}H_{22}N_4OS$, requires 354.1514).

***tert*-butyl (3*R*,5*R*)-3-(2,3-dihydro-1,4-benzodioxin-6-yl)-5-(pyridine-2-amido)piperidine-1-carboxylate ((*R,R*)-33j)**. A pressure vial (100 mL) equipped with a magnetic stirring bar was charged with compound (*R*)-**18a** (2.5 g, 8.19 mmol), silver carbonate (2.26 g, 8.19 mmol), $Pd(OAc)_2$ (184 mg, 0.82 mmol), 6-iodo-2,3-dihydro-1,4-benzodioxine (5.0 g, 19.1 mmol), 2,6-dimethylbenzoic acid (307 mg, 2.05 mmol), and 30 mL *t*-BuOH. The vessel was flushed with argon, sealed with a crimp cap and heated to 120 °C. After 24 h, the reaction vessel was removed from the oil bath, cooled to room temperature, and DCM (50 mL) was added to the reaction mixture. The mixture was thoroughly stirred for 10 min, and the solids were removed by filtration, which was additionally rinsed with DCM (50 mL). The combined filtrates were concentrated under reduced pressure and the residue was purified by Biotage Isolera LPLC to give the title compound (*R,R*)-**33j** (2.36 g, 5.37 mmol, 66%) as a white solid. ^{1}H NMR (400 MHz, DMSO-d_6) δ 8.73 – 8.60 (m, 2H), 8.08 – 7.97 (m, 2H), 7.61 (ddd, *J* = 7.4, 4.7, 1.5 Hz, 1H), 6.83 – 6.68 (m, 3H), 4.32 – 4.16 (m, 4H), 4.09 (d, *J* = 12.2 Hz, 1H), 3.99 – 3.87 (m, 2H), 2.01 – 1.86 (m, 2H), 1.42 (s, 9H). Chiral HPLC (Chiralpak IE-H column, 4.6 mm × 25 cm, 30% EtOH/hexane, 1 mL/min): R_t = 28.43 min, > 99% *ee*.

***N*-[(3*R*,5*R*)-5-(2,3-dihydro-1,4-benzodioxin-6-yl)-1-methylpiperidin-3-yl]pyridine-2-carboxamide ((*R,R*)-34m).** *Step 1*. To a stirred solution of (*R,R*)-**33j** (2.3 g, 5.23 mmol) in DCM was added trifluoroacetic acid (4 mL). The resulting mixture was stirred at ambient temperature for 4 h. Then the solvent was removed under reduced pressure, and the crude product was redissolved in water (50 mL). The solution was basified to pH 10 with 15% aq. NaOH and extracted with EtOAc (80 mL × 3). The combined organic layer was dried over anhydrous Na_2SO_4, filtered, and concentrated in vacuo to give *N*-[(3*R*,5*R*)-5-(2,3-dihydro-1,4-benzodioxin-6-yl)piperidin-3-yl]pyridine-2-carboxamide (1.45 g, 4.27 mmol, 82%) as a pale-yellow solid, which was used without further purification. ^{1}H NMR (400 MHz, DMSO-d_6) δ 8.68 – 8.59 (m, 1H), 8.45 (d, *J* = 8.7 Hz, 1H), 8.08 – 7.92 (m, 2H), 7.60 (ddd, *J* = 7.4, 4.8, 1.5 Hz, 1H), 6.76 (d, *J* = 8.1 Hz, 1H), 6.72 – 6.62 (m, 2H), 4.31 – 4.10 (m, 4H), 4.01 – 3.88 (m, 1H), 3.17 (d, *J* = 3.6 Hz, 1H), 3.07 – 2.95 (m, 1H), 2.94 – 2.84 (m, 1H), 2.69 – 2.58 (m, 1H), 2.48 – 2.38 (m, 2H), 2.33 (t, *J* = 11.7 Hz, 1H), 2.01 – 1.91 (m, 1H), 1.77 (q, *J* = 12.1 Hz, 1H).

Step 2. To a stirred solution of *N*-[(3*R*,5*R*)-5-(2,3-dihydro-1,4-benzodioxin-6-yl)piperidin-3-yl]pyridine-2-carboxamide (1.45 g, 4.27 mmol) and glacial acetic acid (0.1 mL) in methanol (50 mL) was added 37% w/v formaldehyde (0.42 mL). Then sodium triacetoxyborohydride (2.0 g, 9.44 mmol) was added portionwise (0.5 g every 20 min). 2 hours after the final addition, the solvent was removed in vacuo and the residue was partitioned between EtOAc and water. The biphasic solution was extracted twice with EtOAc. Then the combined organics were washed twice with brine, dried

over Na_2SO_4, filtered, and concentrated. Purification of the residue by Biotage Isolera LPLC gave (*R,R*)-**34m** (1.1 g, 3.11 mmol, 73%) as a white solid. ^{1}H NMR (400 MHz, DMSO-d_6) δ 8.64 (dt, *J* = 4.9, 1.3 Hz, 1H), 8.53 (d, *J* = 8.7 Hz, 1H), 8.07 – 7.93 (m, 2H), 7.60 (ddd, *J* = 7.6, 4.7, 1.5 Hz, 1H), 6.81 – 6.66 (m, 3H), 4.28 – 4.17 (m, 4H), 4.15 – 4.02 (m, 1H), 2.91 (dd, *J* = 10.1, 4.1 Hz, 1H), 2.83 – 2.72 (m, 2H), 2.21 (s, 3H), 2.01 – 1.76 (m, 3H), 1.67 (q, *J* = 12.0 Hz, 1H).

(3*R*,5*R*)-5-(2,3-dihydro-1,4-benzodioxin-6-yl)-1-methylpiperidin-3-amine ((*R,R*)-35m). Compound (*R,R*)-**34m** (1.1 g, 3.11 mmol) was suspended in *i*-PrOH (40 mL) in a 100 mL round-bottom flask. NaOH (1.24 g, 31.1 mmol) was added. The reaction mixture was stirred at 85 °C for 18 h. Then the solvent was removed under reduced pressure and water (50 mL) was added. The solution was extracted with EtOAc (50 mL × 2), dried over Na_2SO_4, filtered, and removed the solvent to give the title compound (*R,R*)-**35m** (593 mg, 2.39 mmol, 77%) as a pale-yellow solid without further purification. ^{1}H NMR (400 MHz, DMSO-d_6) δ 6.75 (d, *J* = 8.1 Hz, 1H), 6.71 – 6.60 (m, 2H), 4.28 – 4.13 (m, 4H), 2.84 – 2.59 (m, 4H), 2.15 (s, 3H), 1.89 – 1.78 (m, 1H), 1.67 (t, *J* = 10.7 Hz, 1H), 1.59 – 1.28 (m, 3H), 1.04 (q, *J* = 12.0 Hz, 1H).

3-methyl-2-{[(3*R*,5*R*)-5-phenyl-1-(prop-2-en-1-yl)piperidin-3-yl]amino}-3H,4H,5H-pyrrolo[3,2-d]pyrimidin-4-one ((*R,R*)-36a). *Step1*. To a solution of *N*-[(3*R*,5*R*)-5-phenylpiperidin-3-yl]pyridine-2-carboxamide (800 mg, 2.84 mmol) and Et_3N (324 mg, 3.2 mmol) in MeCN was added 3-bromoprop-1-ene (387 mg, 3.2 mmol). The mixture was reacted at 70 °C for 8 h. After cooling to ambient temperature, the mixture was concentrated and the residue was purified by LPLC to give (*R,R*)-**34a** (690

mg, 2.15 mmol, 76%) as a white solid. ^{1}H NMR (400 MHz, DMSO-d_6) δ 8.67 – 8.61 (m, 1H), 8.57 (d, J = 8.7 Hz, 1H), 8.08 – 7.95 (m, 2H), 7.60 (ddd, J = 7.3, 4.7, 1.5 Hz, 1H), 7.37 – 7.24 (m, 4H), 7.24 – 7.16 (m, 1H), 5.93 – 5.78 (m, 1H), 5.22 – 5.08 (m, 2H), 4.17 – 4.06 (m, 1H), 3.12 – 2.96 (m, 3H), 2.96 – 2.83 (m, 2H), 2.07 – 1.89 (m, 3H), 1.80 (q, J = 12.0 Hz, 1H).

Step 2. (3*R*,5*R*)-1-methyl-5-phenylpiperidin-3-amine ((*R*,*R*)-**35a**) was prepared from (*R*,*R*)-**34a** using the procedure described for (*R*,*R*)-**20a** as colorless oil. The product was used immediately without further purification. LC-MS: *m/z* 191.1 $(M+H)^+$.

Step 3. The title compound (*R*,*R*)-**36a** was prepared from **16** and (*R*,*R*)-**35a** using the procedure described for (*R*,*R*)-**24a** as a white solid. This product was further purified by reverse-phase HPLC. ^{1}H NMR (400 MHz, DMSO-d_6) δ 11.44 (s, 1H), 7.35 – 7.17 (m, 6H), 6.18 – 5.97 (m, 2H), 5.89 – 5.78 (m, 1H), 5.28 – 5.04 (m, 2H), 4.32 – 4.14 (m, 1H), 3.37 (s, 3H), 3.18 (dd, J = 10.5, 4.3 Hz, 1H), 3.05 – 2.84 (m, 4H), 2.11 (dd, J = 12.0, 4.1 Hz, 1H), 1.97 – 1.87 (m, 2H), 1.68 (q, J = 12.7 Hz, 1H).

2-{[(3*R*,5*R*)-1-(2-hydroxyethyl)-5-phenylpiperidin-3-yl]amino}-3-methyl-3H,4H,5H-pyrrolo[3,2-d]pyrimidin-4-one ((*R*,*R*)-36b). The title compound (*R*,*R*)-**36b** was prepared in the same manner as shown for (*R*,*R*)-**36a** except 2-bromoethan-1-ol was used instead. ^{1}H NMR (400 MHz, DMSO-d_6) δ 11.41 (s, 1H), 7.35 – 7.19 (m, 5H), 7.16 (t, J = 2.9 Hz, 1H), 6.06 (t, J = 2.4 Hz, 1H), 6.00 (d, J = 7.8 Hz, 1H), 4.42 (t, J = 5.3 Hz, 1H), 4.25 – 4.14 (m, 1H), 3.57 – 3.48 (m, 2H), 3.36 (s, 3H), 3.18 (dd, J = 10.7, 4.1 Hz, 1H), 2.97 (dd, J = 10.9, 3.7 Hz, 1H), 2.94 – 2.83 (m, 1H), 2.50 – 2.41 (m, 2H), 2.12 – 1.93 (m, 3H), 1.65 (q, J = 12.2 Hz, 1H). ^{13}C NMR (101 MHz, DMSO-d_6) δ

154.48, 149.58, 144.82, 144.19, 128.87, 127.78, 127.51, 126.82, 112.38, 101.18, 60.82, 60.61, 59.12, 58.96, 48.67, 41.74, 37.74, 27.70. HRMS *m*/*z* 368.2083 (M + H^+, $C_{20}H_{25}N_5O_2$, requires 367.2008).

3-methyl-2-{[(3*R*,5*R*)-5-phenyl-1-(2-phenylethyl)piperidin-3-yl]amino}-3H,4H,5H-pyrrolo[3,2-d]pyrimidin-4-one ((*R,R*)-36c). The title compound (*R,R*)-**36b** was prepared in the same manner as shown for (*R,R*)-**36a** except (2-bromoethyl)benzene was used instead. ^{1}H NMR (400 MHz, DMSO-d_6) δ 11.43 (s, 1H), 7.36 – 7.14 (m, 11H), 6.07 (t, *J* = 2.4 Hz, 1H), 6.03 (d, *J* = 7.7 Hz, 1H), 4.30 – 4.12 (m, 1H), 3.37 (s, 3H), 3.32 – 3.26 (m, 1H), 3.01 (dd, *J* = 10.8, 3.6 Hz, 1H), 2.91 (td, *J* = 12.1, 11.5, 3.7 Hz, 1H), 2.82 – 2.69 (m, 2H), 2.62 (t, *J* = 7.8 Hz, 2H), 2.22 – 1.88 (m, 3H), 1.69 (q, *J* = 12.1 Hz, 1H). ^{13}C NMR (101 MHz, DMSO-d_6) δ 154.49, 149.59, 144.85, 144.15, 140.91, 129.20, 128.87, 128.66, 127.81, 127.54, 126.83, 126.25, 112.40, 101.20, 60.42, 60.11, 58.11, 48.75, 41.73, 37.73, 33.10, 27.70. HRMS *m*/*z* 428.2452 (M + H^+, $C_{26}H_{29}N_5O$, requires 427.2372).

2-{[(3*R*,5*R*)-5-(3-bromophenyl)-1-methylpiperidin-3-yl]amino}-3-methyl-3H,4H,5H-pyrrolo[3,2-d]pyrimidin-4-one ((*R,R*)-36d). The title compound (*R,R*)-**36d** was prepared in the same manner as shown for (*R,R*)-**24a** except 1-bromo-3-iodobenzene was used instead. ^{1}H NMR (400 MHz, DMSO-d_6) δ 11.43 (s, 1H), 7.47 (t, *J* = 1.4 Hz, 1H), 7.45 – 7.40 (m, 1H), 7.32 – 7.26 (m, 2H), 7.16 (t, *J* = 2.9 Hz, 1H), 6.05 (t, *J* = 2.4 Hz, 1H), 5.99 (d, *J* = 7.7 Hz, 1H), 4.25 – 4.12 (m, 1H), 3.36 (s, 3H), 3.10 (dd, *J* = 10.5, 4.2 Hz, 1H), 3.01 – 2.83 (m, 2H), 2.23 (s, 3H), 2.13 – 2.03 (m, 1H), 1.91 – 1.76 (m, 2H), 1.61 (q, *J* = 12.2 Hz, 1H). ^{13}C NMR (101 MHz, DMSO-d_6) δ 154.46,

149.53, 146.90, 144.79, 131.07, 130.28, 129.75, 127.78, 126.72, 122.22, 112.41, 101.18, 62.22, 60.35, 48.51, 46.15, 41.22, 36.85, 27.69. HRMS *m*/*z* 416.1082 (M + H^+, $C_{19}H_{22}BrN_5O$, requires 415.1008).

2-{[(3*R*,5*R*)-5-(4-methoxyphenyl)-1-methylpiperidin-3-yl]amino}-3-methyl-3H,4H,5H-pyrrolo[3,2-d]pyrimidin-4-one ((*R,R*)-36e). The title compound (*R,R*)-**36e** was prepared in the same manner as shown for (*R,R*)-**24a** except 1-iodo-4-methoxybenzene was used instead. ^{1}H NMR (400 MHz, DMSO-d_6) δ 11.43 (s, 1H), 7.23 – 7.12 (m, 3H), 6.92 – 6.83 (m, 2H), 6.06 (t, *J* = 2.4 Hz, 1H), 6.00 (d, *J* = 7.7 Hz, 1H), 4.26 – 4.12 (m, 1H), 3.73 (s, 3H), 3.10 (dd, *J* = 10.5, 4.1 Hz, 1H), 2.89 – 2.77 (m, 2H), 2.23 (s, 3H), 2.05 (d, *J* = 11.9 Hz, 1H), 1.82 (dt, *J* = 12.6, 10.6 Hz, 2H), 1.58 (q, *J* = 12.2 Hz, 1H). ^{13}C NMR (101 MHz, DMSO-d_6) δ 158.23, 154.47, 149.58, 144.81, 136.02, 128.36, 127.78, 114.25, 112.40, 101.18, 62.93, 60.42, 55.46, 48.69, 46.20, 40.81, 37.35, 27.71. HRMS *m*/*z* 368.2089 (M + H^+, $C_{20}H_{25}N_5O_2$, requires 367.2008).

2-{[(3*R*,5*R*)-5-(4-butylphenyl)-1-methylpiperidin-3-yl]amino}-3-methyl-3H,4H,5H-pyrrolo[3,2-d]pyrimidin-4-one ((*R,R*)-36f). The title compound (*R,R*)-**36f** was prepared in the same manner as shown for (*R,R*)-**24a** except 1-butyl-4-iodobenzene was used instead. ^{1}H NMR (400 MHz, DMSO-d_6) δ 11.44 (s, 1H), 7.28 – 7.05 (m, 5H), 6.07 (t, J = 2.5 Hz, 1H), 6.00 (d, *J* = 7.8 Hz, 1H), 4.29 – 4.11 (m, 1H), 3.37 (s, 3H), 3.11 (dd, *J* = 10.5, 4.2 Hz, 1H), 2.93 – 2.77 (m, 2H), 2.57 – 2.50 (m, 2H), 2.23 (s, 3H), 2.07 (d, *J* = 12.1 Hz, 1H), 1.91 – 1.75 (m, 2H), 1.67 – 1.48 (m, 3H), 1.38 – 1.20 (m, 2H), 0.88 (t, *J* = 7.3 Hz, 3H). ^{13}C NMR (101 MHz, DMSO-d_6) δ 154.49, 149.57, 144.83, 141.23, 140.71, 128.72, 127.76, 127.28, 112.42, 101.18, 62.77, 60.47, 48.70, 46.22,

41.30, 37.19, 34.88, 33.63, 27.70, 22.22, 14.23. HRMS *m/z* 394.2610 (M + H^+, $C_{23}H_{31}N_5O$, requires 393.2529).

3-methyl-2-{[(3*R*,5*R*)-1-methyl-5-[4-(trifluoromethoxy)phenyl]piperidin-3-yl]amino}-3H,4H,5H-pyrrolo[3,2-d]pyrimidin-4-one ((*R,R*)-36g). The title compound (*R,R*)-**36g** was prepared in the same manner as shown for (*R,R*)-**24a** except 1-iodo-4-(trifluoromethoxy)benzene was used instead. ^{1}H NMR (400 MHz, DMSO-d_6) δ 11.44 (s, 1H), 7.46 – 7.37 (m, 2H), 7.31 (d, *J* = 8.2 Hz, 2H), 7.16 (t, *J* = 2.9 Hz, 1H), 6.06 (t, *J* = 2.4 Hz, 1H), 6.01 (d, *J* = 7.7 Hz, 1H), 4.29 – 4.13 (m, 1H), 3.36 (s, 3H), 3.11 (dd, *J* = 10.5, 4.1 Hz, 1H), 3.04 – 2.94 (m, 1H), 2.87 (dd, *J* = 11.0, 3.6 Hz, 1H), 2.24 (s, 3H), 2.10 (dt, *J* = 12.9, 3.8 Hz, 1H), 1.92 – 1.77 (m, 2H), 1.60 (q, *J* = 12.2 Hz, 1H). ^{13}C NMR (101 MHz, DMSO-d_6) δ 154.46, 149.55, 147.28, 144.79, 143.50, 129.28, 127.77, 121.85, 121.44, 119.30, 112.42, 101.18, 62.32, 60.36, 48.58, 46.17, 40.99, 37.10, 27.70. HRMS *m/z* 422.1832 (M + H^+, $C_{20}H_{22}F_3N_5O_2$, requires 421.1726).

2-{[(3*R*,5*R*)-5-[4-chloro-3-(trifluoromethyl)phenyl]-1-methylpiperidin-3-yl]amino}-3-methyl-3H,4H,5H-pyrrolo[3,2-d]pyrimidin-4-one ((*R,R*)-36h). The title compound (*R,R*)-**36h** was prepared in the same manner as shown for (*R,R*)-**24a** except 1-chloro-4-iodo-2-(trifluoromethyl)benzene was used instead. ^{1}H NMR (400 MHz, DMSO-d_6) δ 11.45 (s, 1H), 7.76 – 7.60 (m, 3H), 7.17 (t, *J* = 2.9 Hz, 1H), 6.06 (t, *J* = 2.4 Hz, 1H), 6.02 (d, *J* = 7.7 Hz, 1H), 4.29 – 4.17 (m, 1H), 3.38 (s, 3H), 3.16 – 3.04 (m, 2H), 2.90 (dd, *J* = 10.9, 3.9 Hz, 1H), 2.25 (s, 3H), 2.12 (dt, *J* = 12.4, 4.0 Hz, 1H), 1.93 – 1.82 (m, 2H), 1.63 (q, *J* = 12.2 Hz, 1H). ^{13}C NMR (101 MHz, DMSO-d_6) δ 154.46, 149.52, 144.77, 144.08, 133.38, 132.14, 129.01, 127.78, 126.87, 126.76,

126.71, 112.43, 101.18, 61.88, 60.24, 48.42, 46.08, 40.74, 36.66, 27.69. HRMS *m*/*z* 440.1476 (M + H^+, $C_{20}H_{21}ClF_3N_5O$, requires 439.1387).

2-{[(3*R*,5*R*)-5-[4-(benzyloxy)phenyl]-1-methylpiperidin-3-yl]amino}-3-methyl-3H,4H,5H-pyrrolo[3,2-d]pyrimidin-4-one ((*R,R*)-36i). The title compound (*R,R*)-**36i** was prepared in the same manner as shown for (*R,R*)-**24a** except 1-(benzyloxy)-4-iodobenzene was used instead. ^{1}H NMR (400 MHz, DMSO-d_6) δ 11.43 (s, 1H), 7.45 – 7.37 (m, 4H), 7.35 – 7.30 (m, 1H), 7.21 – 7.14 (m, 3H), 7.00 – 6.94 (m, 2H), 6.06 (t, *J* = 2.4 Hz, 1H), 5.98 (d, *J* = 7.7 Hz, 1H), 5.07 (s, 2H), 4.25 – 4.12 (m, 1H), 3.36 (s, 3H), 3.13 – 3.05 (m, 1H), 2.87 – 2.76 (m, 2H), 2.22 (s, 3H), 2.09 – 2.01 (m, 1H), 1.86 – 1.74 (m, 2H), 1.57 (q, *J* = 12.3 Hz, 1H). ^{13}C NMR (101 MHz, DMSO-d_6) δ 157.33, 154.48, 149.58, 144.82, 137.70, 136.32, 128.86, 128.39, 128.20, 128.05, 127.76, 115.17, 112.41, 101.19, 69.62, 62.92, 60.46, 48.71, 46.22, 40.84, 37.37, 27.71. HRMS *m*/*z* 444.2394 (M + H^+, $C_{26}H_{29}N_5O_2$, requires 443.2321).

2-{[(3*R*,5*R*)-5-(4-hydroxyphenyl)-1-methylpiperidin-3-yl]amino}-3-methyl-3H,4H,5H-pyrrolo[3,2-d]pyrimidin-4-one ((*R,R*)-36j). A stirred solution of (*R,R*)-**36i** (660 mg, 1.49 mmol) and 10% Pd/C in MeOH was carefully evacuated and backfilled with H_2 atmosphere and finally allowed to stir at ambient temperature overnight with a H_2 balloon attached. Upon reaction completion the suspension was filtered through celite with MeOH washings. The filtrate was then concentrated and the residue was purified by Biotage Isolera LPLC (DCM/MeOH/Et_3N 60:1:0.2- 15:1:0.05) to give (*R,R*)-**36j** (340 mg, 65%) as a white solid. ^{1}H NMR (400 MHz, DMSO-d_6) δ 11.42 (s, 1H), 9.21 (s, 1H), 7.15 (t, *J* = 2.9 Hz, 1H), 7.10 – 7.03 (m, 2H), 6.74 – 6.69

(m, 2H), 6.05 (t, *J* = 2.4 Hz, 1H), 5.99 (d, *J* = 7.7 Hz, 1H), 4.24 – 4.11 (m, 1H), 3.36 (s, 3H), 3.14 – 3.06 (m, 1H), 2.85 – 2.77 (m, 2H), 2.23 (s, 3H), 2.03 (d, *J* = 12.4 Hz, 1H), 1.87 – 1.77 (m, 2H), 1.55 (q, *J* = 12.3 Hz, 1H). ^{13}C NMR (101 MHz, DMSO-d_6) δ 156.24, 154.48, 149.58, 144.81, 134.13, 128.25, 127.78, 115.60, 112.41, 101.18, 62.87, 60.25, 48.64, 46.09, 40.72, 37.38, 27.73. HRMS *m*/*z* 354.1927 (M + H$^+$, $C_{19}H_{23}N_5O_2$, requires 353.1852).

3-methyl-2-{[(3*R*,5*R*)-1-methyl-5-(3-phenylphenyl)piperidin-3-yl]amino}-3H,4H,5H-pyrrolo[3,2-d]pyrimidin-4-one ((*R,R*)-36k). The title compound (*R,R*)-**36k** was prepared in the same manner as shown for (*R,R*)-**24a** except 1-iodo-3-phenylbenzene was used instead. ^{1}H NMR (400 MHz, DMSO-d_6) δ 11.45 (s, 1H), 7.70 – 7.62 (m, 2H), 7.57 – 7.34 (m, 6H), 7.31 – 7.25 (m, 1H), 7.17 (t, *J* = 2.9 Hz, 1H), 6.08 (t, *J* = 2.4 Hz, 1H), 6.01 (d, *J* = 7.8 Hz, 1H), 4.33 – 4.18 (m, 1H), 3.38 (s, 3H), 3.14 (dd, *J* = 10.4, 4.1 Hz, 1H), 3.07 – 2.87 (m, 2H), 2.25 (s, 3H), 2.18 – 2.11 (m, 1H), 1.96 (t, *J* = 10.5 Hz, 1H), 1.85 (t, *J* = 10.5 Hz, 1H), 1.71 (q, *J* = 12.1 Hz, 1H). ^{13}C NMR (101 MHz, DMSO-d_6) δ 154.50, 149.59, 144.85, 144.73, 140.82, 140.80, 129.48, 129.34, 127.85, 127.80, 127.20, 126.62, 126.03, 125.29, 112.43, 101.21, 62.66, 60.47, 48.68, 46.20, 41.72, 37.02, 27.71. HRMS *m*/*z* 414.2290 (M + H$^+$, $C_{25}H_{27}N_5O$, requires 413.2216).

3-methyl-2-{[(3*R*,5*R*)-1-methyl-5-(4-phenoxyphenyl)piperidin-3-yl]amino}-3H,4H,5H-pyrrolo[3,2-d]pyrimidin-4-one ((*R,R*)-36l). The title compound (*R,R*)-**36l** was prepared in the same manner as shown for (*R,R*)-**24a** except 1-iodo-4-phenoxybenzene was used instead. ^{1}H NMR (400 MHz, DMSO-d_6) δ 11.44 (s, 1H),

7.45 – 7.32 (m, 2H), 7.34 – 7.24 (m, 2H), 7.20 – 7.08 (m, 2H), 7.03 – 6.89 (m, 4H), 6.06 (t, J = 2.4 Hz, 1H), 6.00 (d, J = 8.5 Hz, 1H), 4.28 – 4.13 (m, 1H), 3.15 – 3.07 (m, 1H), 2.98 – 2.81 (m, 2H), 2.24 (s, 3H), 2.14 – 2.05 (m, 1H), 1.93 – 1.72 (m, 3H), 1.60 (q, J = 12.1 Hz, 1H). ^{13}C NMR (101 MHz, DMSO-d_6) δ 157.35, 155.48, 154.48, 149.57, 144.81, 139.19, 130.46, 128.96, 127.77, 123.72, 119.15, 118.89, 112.42, 101.19, 62.68, 60.38, 48.66, 46.19, 40.94, 37.27, 27.71. HRMS m/z 430.2237 (M + H$^+$, $C_{25}H_{27}N_5O_2$, requires 429.2165).

3-methyl-2-{[(3*R*,5*R*)-1-methyl-5-(naphthalen-2-yl)piperidin-3-yl]amino}-3H,4H,5H-pyrrolo[3,2-d]pyrimidin-4-one ((*R,R*)-36m). The title compound (*R,R*)-**36m** was prepared in the same manner as shown for (*R,R*)-**24a** except 2-iodonaphthalene was used instead. ^{1}H NMR (400 MHz, DMSO-d_6) δ 11.41 (s, 1H), 7.87 (d, J = 7.8 Hz, 3H), 7.77 (s, 1H), 7.57 – 7.40 (m, 3H), 7.17 (t, J = 2.9 Hz, 1H), 6.12 – 6.00 (m, 2H), 4.31 – 4.19 (m, 1H), 3.37 (s, 3H), 3.19 – 3.03 (m, 2H), 3.00 – 2.92 (m, 1H), 2.27 (s, 3H), 2.22 – 2.12 (m, 1H), 2.00 (t, J = 11.1 Hz, 1H), 1.88 (t, J = 10.5 Hz, 1H), 1.73 (q, J = 12.1 Hz, 1H). ^{13}C NMR (101 MHz, DMSO-d_6) δ 154.50, 149.61, 144.83, 141.63, 133.61, 132.36, 128.27, 127.98, 127.88, 126.61, 126.51, 125.92, 125.30, 112.38, 101.20, 62.44, 60.43, 48.72, 46.23, 41.66, 37.07, 27.73. HRMS m/z 388.2136 (M + H$^+$, $C_{23}H_{25}N_5O$, requires 387.2059).

2-{[(3*R*,5*R*)-5-(2,3-dihydro-1,4-benzodioxin-6-yl)-1-methylpiperidin-3-yl]amino}-3-methyl-3H,4H,5H-pyrrolo[3,2-d]pyrimidin-4-one ((*R,R*)-36n). A solution of DIPEA (183 mg, 1.42 mmol) in NMP (5 mL) was treated with **16** (200 mg, 1.09 mmol) and (*R,R*)-**35m** (325 mg, 1.31 mmol). The resulting mixture was heated to

150 °C and stirred at this temperature for 2 h. After cooling to ambient temperature, the mixture was diluted with water and extracted with EtOAc. The combined organic phase was washed with brine, dried over Na_2SO_4, and concentrated in vacuo. Purification of the residue by Biotage Isolera LPLC gave the title compound (*R,R)*-**36n** (53 mg, 134 mmol, 12%) as a white solid. ^{1}H NMR (400 MHz, DMSO-d_6) δ 11.42 (s, 1H), 7.15 (t, J = 2.9 Hz, 1H), 6.82 – 6.69 (m, 3H), 6.05 (t, J = 2.4 Hz, 1H), 5.98 (d, J = 7.8 Hz, 1H), 4.27 – 4.13 (m, 5H), 3.35 (s, 3H), 3.09 (dd, J = 10.7, 4.3 Hz, 1H), 2.90 – 2.76 (m, 2H), 2.21 (s, 3H), 2.02 (d, J = 10.2, 6.4 Hz, 1H), 1.89 – 1.77 (m, 2H), 1.55 (q, J = 12.2 Hz, 1H). ^{13}C NMR (101 MHz, DMSO-d_6) δ 154.46, 149.55, 144.79, 143.63, 142.31, 137.10, 127.77, 120.08, 117.31, 115.95, 112.40, 101.17, 64.54, 64.44, 62.73, 60.33, 48.55, 46.12, 40.82, 37.17, 27.70. HRMS *m/z* 396.2035 (M + H^+, $C_{21}H_{25}N_5O_3$, requires 395.1957). Chiral HPLC (Chiralpak IE-H column, 4.6 mm × 25 cm, *i*-PrOH/Hexane/EtN_3 = 30: 70: 0.14, 1 mL/min): R_t = 31.54 min, > 99% *ee*.

3-methyl-2-{[(3*S*,5*S*)-1-methyl-5-phenylpiperidin-3-yl]amino}-3H,4H,5H-pyrrolo[3,2-d]pyrimidin-4-one ((*S,S*)-36n). The title compound (*S,S*)-**36n** was prepared as a white solid by the same procedures as (*R,R)*-**36n** except the starting material *tert*-butyl (3*S*)-3-(pyridine-2-amido)piperidine-1-carboxylate (*S*)-**18a** was used instead. ^{1}H NMR (400 MHz, DMSO-d_6) δ 7.43 (d, J = 3.0 Hz, 1H), 6.84 – 6.66 (m, 3H), 6.41 (d, J = 8.1 Hz, 1H), 6.26 (d, J = 3.0 Hz, 1H), 4.46 – 4.30 (m, 1H), 4.21 (s, 4H), 4.01 (s, 3H), 3.31 (s, 3H), 3.11 – 2.96 (m, 1H), 2.91 – 2.74 (m, 2H), 2.24 (s, 3H), 2.04 – 1.79 (m, 3H), 1.69 (q, J = 12.0 Hz, 1H). ^{13}C NMR (101 MHz, DMSO-d_6) δ 151.12, 150.92, 150.33, 143.64, 142.34, 137.01, 135.21, 120.12, 117.30, 115.98,

113.83, 100.49, 64.55, 64.45, 62.48, 59.70, 47.58, 46.14, 40.69, 36.85, 36.73. HRMS *m*/*z* 396.2040 ($M + H^+$, $C_{21}H_{25}N_5O_3$, requires 395.1957). Chiral HPLC (Chiralpak IE-H column, 4.6 mm × 25 cm, *i*-PrOH/Hexane/EtN_3 = 30: 70: 0.14, 1 mL/min): R_t = 21.65 min, > 99% *ee*.

4.2. Protein Expression and Purification. For the isothermal-titration calorimetry (ITC), thermal-shift assay (TSA), and crystallogenesis, human PCAF, GCN5, BRD4(1), ATAD2, BAZ2B, BRD9, BRPF1, BRPF3, EP300, FALZ, TAF1(1), and TRIM24 bromodomains were expressed and purified according to the protocols previously described.[1] All proteins were expressed as *N*-terminal His-tagged fusions and purified using Ni-chelating affinity chromatography. Then these proteins were purified by gel filtration using Superdex200 column, eluted with buffer containing 10 mM HEPES pH 7.5 and 500 mM NaCl, concentrated to 3 mg/mL, and frozen at -80 °C for thermal shift assays. PCAF and GCN5 BRDs were further treated with TEV protease at 4°C overnight to cleave *N*-terminal His-tag. The two proteins were then purified by gel filtration chromatography (Superdex 200; GE-Healthcare), concentrated to 12 mg/mL, flash-frozen in liquid nitrogen, and stored at -80 °C for ITC assays and crystallogenesis.

For the homogeneous time-resolved fluorescence (HTRF) experiments, GST-tagged PCAF was cloned into pET28a vector and overexpressed in Escherichia coli Rosetta (DE3). Purification was carried on GST-affinity resin (Thermo Scientific), and reduced glutathione was used for protein release. GST-PCAF was further purified by gel filtration chromatography on a Superdex 200 column (GE Healthcare) using a buffer of 25 mM HEPES (pH 7.5) and 300 mM NaCl.

4.3. Thermal-Shift Assay (TSA). The TSA experiments were performed at least in duplicate. Proteins were prepared in 10 mM HEPES pH 7.5, 500 mM NaCl, and assayed in low-profile PCR tubes (Bio-Rad, TLS0851) at a final concentration of 2 μM in 20-μL volume. Compounds were added at a final concentration of 10 μM (final concentration 0.1% DMSO). SYPRO Orange dye (Thermo Fisher Scientific) was added at a dilution of 1:1000. The thermal melting experiments were carried using a Bio-Rad CFX96 RT-PCR system. The tubes were first equilibrated at 25 °C for 3 min, then the tubes were heated from 25 to 95 °C with a step of 1 °C/min. Raw fluorescence data were recorded using CFX Maestro, melting temperature shifts were calculated as previously described.[34]

4.4. Isothermal-Titration Calorimetry (ITC). ITC was used to evaluate the thermodynamics parameters of the binding between PCAF bromodomain and all the final compounds. Titrations were carried out on a MicroCal ITC200 microcalorimeter (Malvern Instruments). All experiments were carried out at 25 °C in 25 mM HEPES (pH 7.5), 300 mM NaCl, 0.5 mM TCEP. Compounds were diluted directly in the same batch buffer prior to experiments. Each experiment was designed as reverse titrations experiments (protein in the syringe and ligand in the cell) using an initial injection of 0.4 μL followed by 19 injections of 2 μL. The first injection (generally 0.4 μL) was included in the titration protocol in order to remove air bubbles trapped in the syringe prior to the titration. Background dilution heat was subtracted from each experiment. Thermodynamic parameters were calculated using $\Delta G = \Delta H - T\Delta S = -RT\ln K_A$, where $K_D = 1/K_A$. ΔG, ΔH and ΔS are changes in free energy, enthalpy and entropy respectively. Independent single site binding models were employed in data analysis.

4.5. Homogeneous Time-Resolved Fluorescence (HTRF). HTRF assay was carried out using a Cisbio EPIgeneous Binding Domain Kit B (62BDBPEG) using the

standard assay protocol with GST-PCAF BRD and biotinylated substrate **46**. The protein GST-PCAF BRD was produced and purified in house. The biotinylated substrate **46** was a kind gift from Prof. Dr. P. E. Brennan (Oxford University). The IC_{50} measurements were performed in duplicate. 4 uL GST-PCAF BRD (100 nM), 2 uL tested compounds, 4 uL compound **46** (500 nM), 5 uL SA-XL665 (250 nM), and 5 uL 1×GST Ab-Eu^{3+} were added into a 96-well low-volume plate (Cisbio 66PL96025), then the plate was sealed and incubated at room temperature for 15 hours. Readings were recorded using Cytation Hybrid Multi-Mode Reader with an excitation filter at 337 nm and fluorescence measurement at 620 and 665 nm (60 μs integration delay and 400 μs integration time). The IC_{50} values were normalized and fitted with Prism 7.

4.6. BROMOscan. Bromodomain profiling was provided by DiscoveRx Corp. using their BROMOscan platform (http://www.discoverx.com/).[35] (*R,R)*-**36n** was profiled at 1 μM against 32 recombinant bromodomains.

4.7.Eurofins KinaseProfiler. Kinase profiling was performed by Eurofins (Dundee, U. K., https://www.eurofins.com/). (*R,R*)-**24a**, *endo*-**24c** and (*R,R)*-**36n** were profiled at a single concentration of 10 μM against a panel of 422 kinases.

4.8. Crystallization and Structure Determination. PCAF and GCN5 BRDs were crystallized by vapor diffusion in sitting drops. For PCAF, crystals grew in a mixture of 1 μL protein solution at 16 mg/ ml (25 mM HEPES, pH 7.5, 300 mM NaCl, 0.5 mM TCEP) and 1 μL reservoir solution (100 mM HEPES pH 8.2, 26% PEG10000 (v/v), 4% glycol) at 4 °C. Then overnight soaking of compound **12** was performed. For GCN5, crystals with compound (*R,R)*-**36n** were grown by mixing 1 μL of the protein (12 mg/mL and 4 mM final ligand concentration) with an equal volume of reservoir solution containing 0.2 M ammonium acetate, 0.1 M Tris pH 8.5, 25% w/v polyethylene glycol

3350 at 20 °C. Diffraction quality crystals grew within 5-7 days. All crystals were cryoprotected with reservoir solution supplemented with 20% glycerol (v/v) before being plunge-frozen in liquid nitrogen.

Diffraction data were collected at the Shanghai Synchrotron Light Source (Shanghai, China). Data were indexed, integrated and scaled using HKL2000[36] or XDS.[37] Structures were solved by molecular replacement with Phaser[38] using 5mkx.pdb as template for PCAF bromodomain and 5mlj.pdb as template for GCN5 bromodomain. Initial models were refined alternating cycles of automatic refinement with Phenix.refine[39, 40] and manual model building with WinCOOT 0.8.9.[41] The structure figures were prepared using Pymol. For the data collection and refinement statistics, see Supporting Information Table S4.

4.9. NanoBRET. HEK293T cells (4×10^5/ml) were plated in 6-well plate and co-transfected with Histone H3.3-Halotag and PCAF-Nanoluciferase (Promega). Twenty hours after transfection, cells were digested, collected and exchanged into Phenol red-free DMEM containing 4% FBS. Cell density was adjusted to 2×10^5/ml and then re-plated into a 96-well assay white plate (Corning Costar #3917) in the absence (blank control) or the presence of 100 nM NanoBRET 618 fluorescent ligand (Promega N1661). Compounds or DMSO (vehicle control) were diluted using media and then added into a 96-well plate at indicated concentrations. After that, the 96-well plate was incubated for 18 h at 37 ℃ in the presence of 5% CO_2. NanoBRET Nano-Glo substrate (Promega N1661) was diluted 100 times using media and then added 25 μL to each sample well. Readings were recorded within 10 minutes using Thermo Scientific Varioskan LUX equipped with 460/80 nm bandpass and 610 nm longpass filter module. The corrected BRET ratio was calculated as the following formula: NanoBRET corrected ratio = Ligand (610 nm/460 nm) – blank control (610 nm/460 nm) BRET

ratios are expressed as milliBRET units (mBU), where 1 mBU corresponds to the corrected BRET ratio multiplied by 1000.

4.10. RNA-seq. Total RNA was extracted using the TRIzol reagent according to the manufacturer's protocol. RNA purity and quantification were evaluated using a NanoDrop 2000 spectrophotometer (Thermo Scientific, USA). RNA integrity was assessed using the Agilent 2100 Bioanalyzer (Agilent Technologies, Santa Clara, CA, USA). Then the libraries were constructed using TruSeq Stranded mRNA LT Sample Prep Kit (Illumina, San Diego, CA, USA) according to the manufacturer's instructions. The transcriptome sequencing and analysis were conducted by OE Biotech Co., Ltd. (Shanghai, China).

The libraries were sequenced on an Illumina HiSeq X Ten platform and 150 bp paired-end reads were generated. Raw data (raw reads) of fastq format were firstly processed using Trimmomatic. After removing low quality reads and reads containing adapter or ploy-N from raw data, the clean reads were mapped to the human genome using HISAT2.

FPKM value of each gene was calculated using Cufflinks, and the read counts of each gene were obtained by HTSeq-count. Differential expression analysis was performed using the DESeq (2012) R package. P value < 0.05 and fold change > 1.5 or < 1/1.5 was set as the threshold for significantly differential expression.

4.11. Microsomal Stability Assay. (*R,R*)-**36n** (1 μM) was incubated with 0.5 mg/mL human liver microsomes. NADPH was maintained at 1 mM in 1000 μL of reaction volume. The reaction was then evaluated at 0, 5, 15, 30, and 45 min and was terminated by the addition of acetonitrile. Samples were centrifuged for 15 min at 6000

rpm and the supernatant analyzed using LC-MS. Percentage parent remaining was calculated considering percent parent area at 0 min as 100%.

4.12. Plasma protein binding. Plasma protein binding was measured using previously published protocol.[42]

4.13. Rats pharmacokinetic studies. Animal studies were conducted under the approval of the Experimental Animal Management Committee of Sichuan University. The pharmacokinetics analysis of (*R,R*)-**36n** was conducted in male Sprague−Dawley rats. The 6 to 8 week old Sprague-Dawley rats were treated with a single dose of (*R,R*)-**36n** at 10 mg/kg by intravenous tail vein injection and oral gavage administration (2.5% (v/v) ethanol and 2.5% tween-80 in saline, pH 7.0). Serial blood samples (200 μL) were collected from jugular vein at designated times. Blood samples were put on ice and centrifuged to obtain plasma samples (6800 × g, 6 min under 4 ℃) within 2 hours. All blood samples were stored at approximately at -80 °C until analysis.

The blood samples were prepared for analysis by placing a 20 μL aliquot into a 96-well plate followed by the addition of 400 μL MeOH of acetonitrile containing 100 ng/mL IS. The mixture was vortexed for 1 min and centrifuged at 18000 × g for 7 min. An aliquot of 1 μL supernatant was injected for LC-MS/MS analysis. Noncompartmental pharmacokinetic parameters were fitted using DAS software (Enterprise, version 2.0, Mathematical Pharmacology Professional Committee of China).

ASSOCIATED CONTENT

Supporting Information

Flowchart of hits identification against PCAF bromodomain; DSF results of test compounds against a panel of 12 bromodomains; BROMOscan assay of (*R*,*R*)-**36n** against 32 bromodomains; Kinase inhibition profiles of (*R,R*)-**24a**, *endo*-**24c** and (*R,R*)-**36n**; ITC curves of selected compounds against PCAF; X-ray data collection and refinement statistics; ^{1}H spectra, ^{13}C NMR spectra; HRMS spectra; chiral HPLC traces (PDF).

Molecular formula strings (CSV)

Accession Codes

Atomic coordinates and structure factors have been deposited in the Protein Data Bank under the following accession codes: 6J3O (PCAF/compound **12**), 6J3P (GCN5/compound (*R,R)*-**36n**). Authors will release the atomic coordinates and experimental data upon article publication.

AUTHOR INFORMATION

Corresponding Author

*Tel.: +86-28-85164063; Fax: +86-28-85164060; E-mail: yangsy@scu.edu.cn (S.Y.)

ORCID

Shengyong Yang: 0000-0001-5147-3746

Author Contributions

# L. H., H. L., and L. L. contributed equally to this work.

Notes

The authors declare no competing financial interest.

ACKNOWLEDGEMENTS

This work was supported by the National Natural Science Foundation of China (81573349, 81773633, and 21772130), National Science and Technology Major Project (2018ZX09711002-014-002, 2018ZX09711002-011-019, and 2018ZX09711003-003-006), and 1.3.5 project for disciplines of excellence, West China Hospital, Sichuan University. The authors thank the staff from BL17U1, BL18U, BL19U1 beamlines of National Facility for Protein Science Shanghai (NFPS) at Shanghai Synchrotron Radiation Facility for assistance during data collection.

ABBREVIATIONS USED

BET, bromodomain and extra terminal domain; HAT, histone acetyltransferase; BRD4(1), bromodomain containing protein 4, first bromodomain; S_NAr, nucleophilic aromatic substitution; BRD9, bromodomain containing protein 9; BAZ2, bromodomain adjacent to zinc finger domain 2; BRPF, bromodomain and PHD finger; CECR2, cat eye syndrome chromosome region, candidate 2; FALZ, fetal Alzheimer-50 clone 1 protein; TAF1, TBP-associated factor RNA polymerase 1; EP300, E1A-binding protein, 300 kDa; DSF, differential scanning fluorimetry; GCN5, general control nonderepressible 5; KAT2, lysine acetyl-transferase 2; PCAF, p300/CBPassociated factor; HTRF, homogeneous time-Resolved fluorescence; ITC, isothermal titration calorimetry; DMAP, 4-Dimethylaminepyridine; RNA-seq, RNA-sequencing

REFERENCES

1. Filippakopoulos, P.; Picaud, S.; Mangos, M.; Keates, T.; Lambert, J. P.; Barsyte-

Lovejoy, D.; Felletar, I.; Volkmer, R.; Muller, S.; Pawson, T.; Gingras, A. C.; Arrowsmith, C. H.; Knapp, S. Histone recognition and large-scale structural analysis of the human bromodomain family. *Cell* **2012,** 149, 214-231.

2. Filippakopoulos, P.; Knapp, S. Targeting bromodomains: epigenetic readers of lysine acetylation. *Nat Rev Drug Discov* **2014,** 13, 337-356.

3. Romero, F. A.; Taylor, A. M.; Crawford, T. D.; Tsui, V.; Cote, A.; Magnuson, S. Disrupting acetyl-lysine recognition: progress in the development of bromodomain inhibitors. *J Med Chem* **2016,** 59, 1271-1298.

4. Liu, Z.; Wang, P.; Chen, H.; Wold, E. A.; Tian, B.; Brasier, A. R.; Zhou, J. Drug discovery targeting bromodomain-containing protein 4. *J Med Chem* **2017,** 60, 4533-4558.

5. Dawson, M. A.; Prinjha, R. K.; Dittmann, A.; Giotopoulos, G.; Bantscheff, M.; Chan, W.-I.; Robson, S. C.; Chung, C.-w.; Hopf, C.; Savitski, M. M.; Huthmacher, C.; Gudgin, E.; Lugo, D.; Beinke, S.; Chapman, T. D.; Roberts, E. J.; Soden, P. E.; Auger, K. R.; Mirguet, O.; Doehner, K.; Delwel, R.; Burnett, A. K.; Jeffrey, P.; Drewes, G.; Lee, K.; Huntly, B. J. P.; Kouzarides, T. Inhibition of BET recruitment to chromatin as an effective treatment for MLL-fusion leukaemia. *Nature* **2011,** 478, 529-533.

6. Delmore, J. E.; Issa, G. C.; Lemieux, M. E.; Rahl, P. B.; Shi, J.; Jacobs, H. M.; Kastritis, E.; Gilpatrick, T.; Paranal, R. M.; Qi, J.; Chesi, M.; Schinzel, A. C.; McKeown, M. R.; Heffernan, T. P.; Vakoc, C. R.; Bergsagel, P. L.; Ghobrial, I. M.; Richardson, P. G.; Young, R. A.; Hahn, W. C.; Anderson, K. C.; Kung, A. L.; Bradner, J. E.; Mitsiades, C. S. BET bromodomain inhibition as a therapeutic strategy to target

c-Myc. *Cell* **2011,** 146, 904-917.

7. Nicodeme, E.; Jeffrey, K. L.; Schaefer, U.; Beinke, S.; Dewell, S.; Chung, C. W.; Chandwani, R.; Marazzi, I.; Wilson, P.; Coste, H.; White, J.; Kirilovsky, J.; Rice, C. M.; Lora, J. M.; Prinjha, R. K.; Lee, K.; Tarakhovsky, A. Suppression of inflammation by a synthetic histone mimic. *Nature* **2010,** 468, 1119-1123.

8. Picaud, S.; Wells, C.; Felletar, I.; Brotherton, D.; Martin, S.; Savitsky, P.; Diez-Dacal, B.; Philpott, M.; Bountra, C.; Lingard, H.; Fedorov, O.; Muller, S.; Brennan, P. E.; Knapp, S.; Filippakopoulos, P. RVX-208, an inhibitor of BET transcriptional regulators with selectivity for the second bromodomain. *Proc Natl Acad Sci USA* **2013,** 110, 19754-19759.

9. Shu, S.; Lin, C. Y.; He, H. H.; Witwicki, R. M.; Tabassum, D. P.; Roberts, J. M.; Janiszewska, M.; Huh, S. J.; Liang, Y.; Ryan, J.; Doherty, E.; Mohammed, H.; Guo, H.; Stover, D. G.; Ekram, M. B.; Brown, J.; D'Santos, C.; Krop, I. E.; Dillon, D.; McKeown, M.; Ott, C.; Qi, J.; Ni, M.; Rao, P. K.; Duarte, M.; Wu, S. Y.; Chiang, C. M.; Anders, L.; Young, R. A.; Winer, E.; Letai, A.; Barry, W. T.; Carroll, J. S.; Long, H.; Brown, M.; Liu, X. S.; Meyer, C. A.; Bradner, J. E.; Polyak, K. Response and resistance to BET bromodomain inhibitors in triple-negative breast cancer. *Nature* **2016,** 529, 413-417.

10. Theodoulou, N. H.; Tomkinson, N. C.; Prinjha, R. K.; Humphreys, P. G. Progress in the development of non-BET bromodomain chemical probes. *ChemMedChem* **2016,** 11, 477-487.

11. Moustakim, M.; Clark, P. G. K.; Hay, D. A.; Dixon, D. J.; Brennan, P. E. Chemical

probes and inhibitors of bromodomains outside the BET family. *Medchemcomm* **2016,** 7, 2246-2264.

12. Clegg, M. A.; Tomkinson, N. C. O.; Prinjha, R. K.; Humphreys, P. G. Advancements in the development of non-BET bromodomain chemical probes. *ChemMedChem* **2019,** 14, 362-385.

13. Lau, O. D.; Courtney, A. D.; Vassilev, A.; Marzilli, L. A.; Cotter, R. J.; Nakatani, Y.; Cole, P. A. P300/CBP-associated factor histone acetyltransferase processing of a peptide substrate. Kinetic analysis of the catalytic mechanism. *J Biol Chem* **2000,** 275, 21953-21959.

14. Linares, L. K.; Kiernan, R.; Triboulet, R.; Chable-Bessia, C.; Latreille, D.; Cuvier, O.; Lacroix, M.; Le Cam, L.; Coux, O.; Benkirane, M. Intrinsic ubiquitination activity of PCAF controls the stability of the oncoprotein Hdm2. *Nat Cell Biol* **2007,** 9, 331-338.

15. Mujtaba, S.; He, Y.; Zeng, L.; Farooq, A.; Carlson, J. E.; Ott, M.; Verdin, E.; Zhou, M. M. Structural basis of lysine-acetylated HIV-1 Tat recognition by PCAF bromodomain. *Mol Cell* **2002,** 9, 575-586.

16. Wang, T.; Yao, W.; Shao, Y.; Zheng, R.; Huang, F. PCAF fine-tunes hepatic metabolic syndrome, inflammatory disease, and cancer. *J Cell Mol Med* **2018,** 22, 5787-5800.

17. Zeng, L.; Li, J.; Muller, M.; Yan, S.; Mujtaba, S.; Pan, C.; Wang, Z.; Zhou, M. M. Selective small molecules blocking HIV-1 Tat and coactivator PCAF association. *J Am Chem Soc* **2005,** 127, 2376-2377.

18. Hu, P.; Wang, X.; Zhang, B.; Zhang, S.; Wang, Q.; Wang, Z. Fluorescence polarization for the evaluation of small-molecule inhibitors of PCAF BRD/Tat-AcK50 association. *ChemMedChem* **2014,** 9, 928-931.

19. Navratilova, I.; Aristotelous, T.; Picaud, S.; Chaikuad, A.; Knapp, S.; Filappakopoulos, P.; Hopkins, A. L. Discovery of new bromodomain scaffolds by biosensor fragment screening. *ACS Med Chem Lett* **2016,** 7, 1213-1218.

20. Chaikuad, A.; Lang, S.; Brennan, P. E.; Temperini, C.; Fedorov, O.; Hollander, J.; Nachane, R.; Abell, C.; Muller, S.; Siegal, G.; Knapp, S. Structure-based identification of inhibitory fragments targeting the p300/CBP-associated factor bromodomain. *J Med Chem* **2016,** 59, 1648-1653.

21. Albrecht, B. K.; Cote, A.; Crawford, T.; Duplessis, M.; Good, A. C.; Leblanc, Y.; Magnuson, S.; Nasveschuk, C. G.; Pastor, R.; Romero, F. A.; Taylor, A. M. Therapeutic Compounds and Uses Thereof. WO 2016/036873 A1, 2016.

22. Albrecht, B. K.; Cote, A.; Crawford, T.; Duplessis, M.; Good, A. C.; Leblanc, Y.; Magnuson, S.; Nasveschuk, C. G.; Pastor, R.; Romero, F. A.; Taylor, A. M. Phthalazine Derivatives of Forumula (I) as PCAF and GCN5 Inhibitors for Use in the Treatment of Cancer. WO 2016/036954 A1, 2016.

23. Albrecht, B. K.; Burdick, D. J.; Cote, A.; Duplessis, M.; Nasveschuk, C. G.; Taylor, A. M. Pyridazinone Derivatives and Their Use in the Treatment of Cancer. WO 2016/112298 A1, 2016.

24. Moustakim, M.; Clark, P. G.; Trulli, L.; Fuentes de Arriba, A. L.; Ehebauer, M. T.; Chaikuad, A.; Murphy, E. J.; Mendez-Johnson, J.; Daniels, D.; Hou, C. D.; Lin, Y. H.;

Walker, J. R.; Hui, R.; Yang, H.; Dorrell, L.; Rogers, C. M.; Monteiro, O. P.; Fedorov, O.; Huber, K. V.; Knapp, S.; Heer, J.; Dixon, D. J.; Brennan, P. E. Discovery of a PCAF bromodomain chemical probe. *Angew Chem Int Ed* **2017,** 56, 827-831.

25. Humphreys, P. G.; Bamborough, P.; Chung, C. W.; Craggs, P. D.; Gordon, L.; Grandi, P.; Hayhow, T. G.; Hussain, J.; Jones, K. L.; Lindon, M.; Michon, A. M.; Renaux, J. F.; Suckling, C. J.; Tough, D. F.; Prinjha, R. K. Discovery of a potent, cell penetrant, and selective P300/CBP-associated factor (PCAF)/general control nonderepressible 5 (GCN5) bromodomain chemical probe. *J Med Chem* **2017,** 60, 695-709.

26. Bassi, Z. I.; Fillmore, M. C.; Miah, A. H.; Chapman, T. D.; Maller, C.; Roberts, E. J.; Davis, L. C.; Lewis, D. E.; Galwey, N. W.; Waddington, K. E.; Parravicini, V.; Macmillan-Jones, A. L.; Gongora, C.; Humphreys, P. G.; Churcher, I.; Prinjha, R. K.; Tough, D. F. Modulating PCAF/GCN5 immune cell function through a PROTAC approach. *ACS Chem Biol* **2018,** 13, 2862-2867.

27. Hay, D. A.; Rogers, C. M.; Fedorov, O.; Tallant, C.; Martin, S.; Monteiro, O. P.; Müller, S.; Knapp, S.; Schofield, C. J.; Brennan, P. E. Design and synthesis of potent and selective inhibitors of BRD7 and BRD9 bromodomains. *MedChemComm* **2015,** 6, 1381-1386.

28. Chen, P.; Chaikuad, A.; Bamborough, P.; Bantscheff, M.; Bountra, C.; Chung, C.-w.; Fedorov, O.; Grandi, P.; Jung, D.; Lesniak, R.; Lindon, M.; Müller, S.; Philpott, M.; Prinjha, R.; Rogers, C.; Selenski, C.; Tallant, C.; Werner, T.; Willson, T. M.; Knapp, S.; Drewry, D. H. Discovery and characterization of GSK2801, a selective chemical

probe for the bromodomains BAZ2A and BAZ2B. *J Med. Chem.* **2015,** 59, 1410-1424.

29. Xiang, Q.; Wang, C.; Zhang, Y.; Xue, X.; Song, M.; Zhang, C.; Li, C.; Wu, C.; Li, K.; Hui, X.; Zhou, Y.; Smaill, J. B.; Patterson, A. V.; Wu, D.; Ding, K.; Xu, Y. Discovery and optimization of 1-(1H-indol-1-yl)ethanone derivatives as CBP/EP300 bromodomain inhibitors for the treatment of castration-resistant prostate cancer. *Eur J Med Chem* **2018,** 147, 238-252.

30. Unzue, A.; Zhao, H.; Lolli, G.; Dong, J.; Zhu, J.; Zechner, M.; Dolbois, A.; Caflisch, A.; Nevado, C. The "gatekeeper" residue influences the mode of binding of acetyl indoles to bromodomains. *J Med Chem* **2016,** 59, 3087-3097.

31. Van Steijvoort, B. F.; Kaval, N.; Kulago, A. A.; Maes, B. U. W. Remote functionalization: palladium-catalyzed C5(sp3)-H arylation of 1-boc-3-aminopiperidine through the use of a bidentate directing group. *ACS Catalysis* **2016,** 6, 4486-4490.

32. Crawford, T. D.; Tsui, V.; Flynn, E. M.; Wang, S.; Taylor, A. M.; Cote, A.; Audia, J. E.; Beresini, M. H.; Burdick, D. J.; Cummings, R.; Dakin, L. A.; Duplessis, M.; Good, A. C.; Hewitt, M. C.; Huang, H. R.; Jayaram, H.; Kiefer, J. R.; Jiang, Y.; Murray, J.; Nasveschuk, C. G.; Pardo, E.; Poy, F.; Romero, F. A.; Tang, Y.; Wang, J.; Xu, Z.; Zawadzke, L. E.; Zhu, X.; Albrecht, B. K.; Magnuson, S. R.; Bellon, S.; Cochran, A. G. Diving into the water: inducible binding conformations for BRD4, TAF1(2), BRD9, and CECR2 bromodomains. *J Med Chem* **2016,** 59, 5391-5402.

33. Machleidt, T.; Woodroofe, C. C.; Schwinn, M. K.; Mendez, J.; Robers, M. B.; Zimmerman, K.; Otto, P.; Daniels, D. L.; Kirkland, T. A.; Wood, K. V. NanoBRET--a

novel BRET platform for the analysis of protein-protein interactions. *ACS Chem Biol* **2015,** 10, 1797-1804.

34. Niesen, F. H.; Berglund, H.; Vedadi, M. The use of differential scanning fluorimetry to detect ligand interactions that promote protein stability. *Nat Protoc* **2007,** 2, 2212-2221.

35. Quinn, E.; Wodicka, L.; Ciceri, P.; Pallares, G.; Pickle, E.; Torrey, A.; Floyd, M.; Hunt, J.; Treiber, D. BROMOscan a high throughput, quantitative ligand binding platform identifies best-in-class bromodomain inhibitors from a screen of mature compounds targeting other protein classes. *Cancer Res.* **2013,** 73, 4238.

36. Otwinowski, Z.; Minor, W. Processing of X-ray diffraction data collected in oscillation mode. *Method Enzymol* **1997,** 276, 307-326.

37. Kabsch, W. Xds. *Acta Crystallogr D Biol Crystallogr* **2010,** 66, 125-132.

38. McCoy, A. J.; Grosse-Kunstleve, R. W.; Adams, P. D.; Winn, M. D.; Storoni, L. C.; Read, R. J. Phaser crystallographic software. *J Appl Crystallogr* **2007,** 40, 658-674.

39. Adams, P. D.; Afonine, P. V.; Bunkoczi, G.; Chen, V. B.; Davis, I. W.; Echols, N.; Headd, J. J.; Hung, L. W.; Kapral, G. J.; Grosse-Kunstleve, R. W.; McCoy, A. J.; Moriarty, N. W.; Oeffner, R.; Read, R. J.; Richardson, D. C.; Richardson, J. S.; Terwilliger, T. C.; Zwart, P. H. PHENIX: a comprehensive Python-based system for macromolecular structure solution. *Acta Crystallogr D Biol Crystallogr* **2010,** 66, 213-221.

40. Afonine, P. V.; Grosse-Kunstleve, R. W.; Echols, N.; Headd, J. J.; Moriarty, N. W.; Mustyakimov, M.; Terwilliger, T. C.; Urzhumtsev, A.; Zwart, P. H.; Adams, P. D.

Towards automated crystallographic structure refinement with phenix.refine. *Acta Crystallogr D Biol Crystallogr* **2012,** 68, 352-367.

41. Emsley, P.; Lohkamp, B.; Scott, W. G.; Cowtan, K. Features and development of Coot. *Acta Crystallogr D* **2010,** 66, 486-501.

42. Mitchell, L. H.; Boriack-Sjodin, P. A.; Smith, S.; Thomenius, M.; Rioux, N.; Munchhof, M.; Mills, J. E.; Klaus, C.; Totman, J.; Riera, T. V.; Raimondi, A.; Jacques, S. L.; West, K.; Foley, M.; Waters, N. J.; Kuntz, K. W.; Wigle, T. J.; Scott, M. P.; Copeland, R. A.; Smith, J. J.; Chesworth, R. Novel oxindole sulfonamides and sulfamides: EPZ031686, the first orally bioavailable small molecule SMYD3 inhibitor. *ACS Med Chem Lett* **2016,** 7, 134-138.

Table of Contents Graphic

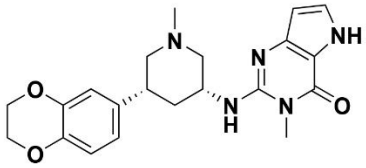

(*R,R*)-**36n**

PCAF
HTRF IC_{50} = 7 nM
ITC K_D = 78 nM